DEWATERING OF AQUACULTURE SLUDGE BY CENTRIFUGATION

by

Alex Mann

BScE in Chemical Engineering, University of New Brunswick, 2021

A Thesis Submitted in Partial Fulfillment
of the Requirements for the Degree of

Master of Science in Engineering

in the Graduate Academic Unit of Chemical Engineering

Supervisor: Michel Couturier, PhD, Chemical Engineering

Examining Board: Guida Bendrich, PhD, Chemical Engineering
Laura Romero-Zeron, PhD, Chemical Engineering
Phil Garland, PhD, Mechanical Engineering

This thesis is accepted by the
Dean of Graduate Studies

THE UNIVERSITY OF NEW BRUNSWICK

June, 2023

ABSTRACT

Currently, aquaculture sludge is shipped offsite for disposal. The disposal cost is directly proportional to the weight of the sludge, which typically has a solids content between 3 to 10 wt.% solids. This has created a strong incentive to remove water from aquaculture sludge in order to reduce its weight and one method to achieve this is centrifugation.

When using a centrifuge, it was determined that aquaculture sludge can be dewatered to 19.3 ± 0.7 wt.% solids. The addition of dewatering aids such as coagulants, flocculants, and sawdust proved to be ineffective at further decreasing the water content in the sludge. Incineration was also investigated as an alternative disposal method for dewatered sludge. The higher heating value of aquaculture sludge was determined the be 16.3 ± 0.2 kJ/g of dry solids and thermodynamic calculations show that sludge must be at least 31 wt.% solids for self-sustained combustion at 800°C.

ACKNOWLEDGEMENTS

I am grateful to my family, friends, workers of UNB and Cooke Aquaculture, and all others who have supported or helped me during my graduate studies. A special thanks go out to my supervisor Dr. Michel Couturier. Without his guidance and expertise, this project would not have been possible.

I personally want to express my gratitude to Cooke Aquaculture and Mitacs for funding this project. I would like also to thank Cooke Aquaculture for allowing me to use their commercial facilities for research purposes.

Table of Contents

List of Tables

List of Figures

List of Symbols, Nomenclature or Abbreviations

List of Abbreviations

CHNS – Carbon, Hydrogen, Nitrogen, and Sulfur

FAU – Formazine Attenuation Unit

FS – Ferric Sulfate ($FeSO_4$)

HHV – Higher Heating Value

PPM – Parts per Million

PAC – Poly-Aluminium Chloride $Al_5(OH)_6Cl_9$

PAM – Polyacrylamide $(C_3H_5NO)_n$

RAS – Recirculating Aquaculture System

RPM – Rotations per Minute

TSS – Total Suspended Solids

US gal – United States Gallon

US gpm – United States Gallons per Minute

WAS – Waste Activated Sludge

List of Symbols

a_e – external acceleration (m/s^2)

A_p – Particle area (m^2)

b – Amount of diatomic oxygen (moles)

c – Amount of carbon (moles)

C – Concentration (kg/m^3)

C_i – Initial concentration (kg/m^3)

C_f – Final concentration (kg/m^3)

$\bar{C}_p$ – Average specific heat capacity (kJ/kg·°C)

d_p – Particle diameter (m)

E – Energy (kJ)

E_{system} – Energy equivalent of the bomb calorimeter (kJ/°C)

F_B – Buoyant force

F_c – Centrifugal force (N)

F_D – Drag force (N)

g – Gravitational acceleration (m/s^2)

h – Amount of hydrogen (moles)

ΔH – Change in enthalpy (kJ)

ΔH_1 – Change in enthalpy from combustion (kJ)

ΔH_2 – Change in enthalpy from evaporation (kJ)

ΔH_3 – Change in enthalpy from products heating (kJ)

h – Specific enthalpy (kJ/kg)

HHV – Higher heating value (kJ/g)

H_{wire} – Correction for heat of combustion of the ignition wire (kJ / cm)

K – Sedimentation constant (m^{-2}·s^{-2})

K_2 – Centrifuge geometry and flowrate constant (s)

L_{wire} – Length of ignition wire ignited (cm)

L – Length of centrifuge (m)

m – Mass (kg)

$\dot{m}$ – Mass flowrate (kg/s)

n – Amount of nitrogen (moles)

$\Delta\rho$ – Difference between the solid and liquid density (kg/m^3)

ρ – Liquid density (kg/m^3)

ρ_p – Particle density (kg/m^3)

q – Flowrate (m^3/s)

Q_{sample} – Energy released by the sample (kJ)

Q_{system} – Energy gained by the bomb calorimeter system (kJ)

Q_{wire} – Energy released by the ignition wire (kJ)

r or r_1 – Inner radius of the cake (m)

r_c – Outer radius of the feed cone (m)

r_i – Inner radius of the weir (m)

r_o or r_3– Outer radius of the basket centrifuge (m)

RCF – Relative centrifugal force (G-Force)

Re – Reynolds number (dimensionless)

s – Amount of sulfur (moles)

μ – Liquid viscosity (Pa·s)

ΔT = Change in temperature (°C)

T_0 – Initial temperature (°C)

T_f – Final temperature (°C)

u – Settling velocity (m/s)

u_t – Terminal settling velocity (m/s)

v – Specific kinetic energy (kJ/kg)

ω – Angular velocity (rad/s)

w – Amount of water (moles)

x – Amount of oxygen (moles)

z – Specific potential energy (kJ/kg)

List of Nomenclature

$CaCO_3$ – Calcium carbonate

CO_2 – Carbon dioxide

HCl – Hydrochloric acid

H_2O – Water

IPA – Isopropyl alcohol

N_2 – Diatomic nitrogen

NO – Nitric oxide

O_2 – Diatomic oxygen

Salmon – *Salmo salar* (atlantic salmon)

SO_2 – Sulfur dioxide

wt.% – Weight percent

Chapter 1: Introduction

1.1 Importance of Aquaculture

Fueled by the increasing population, wealth, and urbanization, the aquaculture sector has grown tremendously over the past 30 years and is the fastest growing food sector in the world (CAIA, 2018). Aquaculture still only provides 50% of the total fish production which is projected to increase from 174 million tonnes in 2018 to 204 million tonnes by 2030 (CAIA, 2018) (FOA, 2020). However, 34% of fish stock are intensely overfished and being removed from the wild at a rate that cannot be replenished naturally (FOA, 2020). While aquaculture proves to be a much more sustainable method of seafood production than wild caught fish, the growth in aquaculture production comes with increases in waste-solids production from the industry. Waste-solids disposal need to be well managed to avoid detrimental effects on the environmental and the economical sustainability of the aquaculture industry.

1.2 Recirculating Aquaculture System

Land-based aquaculture can be categorized into three systems: ponds, flow-through systems, and recirculating aquaculture systems (RAS) (FOA, 2020) (Yeo, Binkowski, & Morris, 2004). Pond culture is when manmade or natural ponds are used to raise fish. Due to the little to no discharge, pond culture must rely on internal natural processes to maintain water quality and as a result, can only support a low mass of fish to volume of water. This is known as semi-intensive aquaculture. A flow-through system consists of diverting a high flow of water from a natural body of water to shallow tanks and then

discharging the water after use. Flow-through systems maintain water quality by continuously discharging and replacing the water and can be operated at a moderate to high intensity (Yeo, Binkowski, & Morris, 2004). A RAS reuses water by treating and continually circulating the water through the system, with only a small percentage discharged and replaced with clean make-up water. A block flow diagram for a typical RAS can be seen in Figure 1-1. In a RAS, fish are grown in large indoor tanks which allow operators to monitor and maintain maximum control of the temperature, pH, salinity, chemical composition, and dissolved oxygen in the system (Martins, et al., 2010) (Yeo, Binkowski, & Morris, 2004). Capital costs for RAS facilities can be high, so in order to be economically viable, RAS are run at a much higher intensity than other methods meaning more fish are produced with less water (Timmons, Ebeling, Wheaton, Summerfelt, & Vinci, 2001). RAS are preferred over other land-based aquaculture methods because of the reduced environmental impact caused by their reduced water usage. This allows RAS to discharge less polluted wastewater and as a result, the amount of make-up water needed is small enough that it can be taken from the aquifer, which is a clean source of freshwater (Yeo, Binkowski, & Morris, 2004) (Timmons, Ebeling, Wheaton, Summerfelt, & Vinci, 2001).

Before the water is recirculated back into the tank in a RAS, waste-solids and harmful compounds are removed by water treatment unit operations before they can reach concentrations that are harmful to the fish. After the water leaves the fish tanks, the solids must be removed immediately because they can negatively impact the rest of the unit operations, and this can be done by filtration, flotation, and settling. Next, a biofilter is used to convert harmful ammonia-nitrogen to a much less harmful nitrate-nitrogen.

Carbon dioxide (CO_2) is then stripped out of the water by an aeration process and an oxygenation system adds dissolved oxygen into the water. Before the water is sent back for use in the tanks, it is disinfected by ozone or ultraviolet light. RAS use less water, discharge less pollutants into the environment and use less land compared to the other land-based aquaculture methods. In spite of the fact that RAS are more environmentally friendly, this comes at the expense of a higher capital cost, and difficulty to operate compared to flow-through and pond culture (Timmons, Ebeling, Wheaton, Summerfelt, & Vinci, 2001).

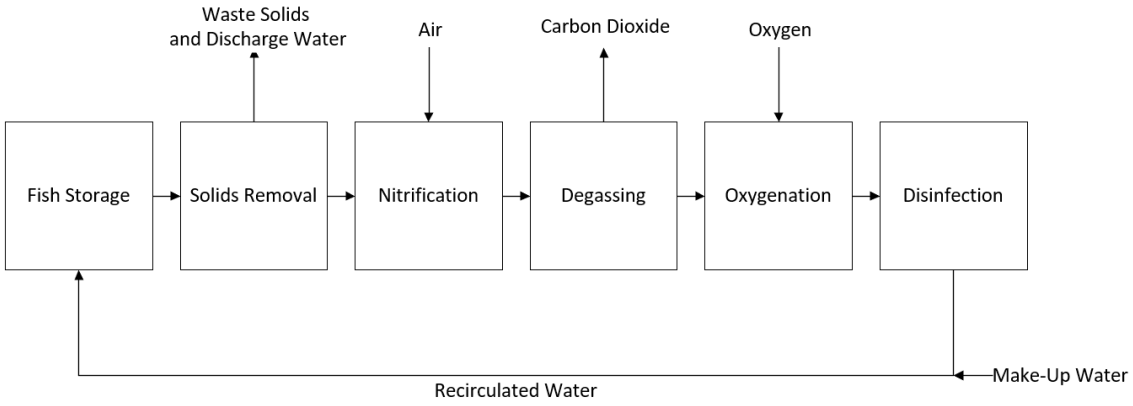

Figure 1-1: Conventional RAS block flow diagram.

The efficiency of a RAS is measured by its water exchange rate which is influenced by the discharge rate. Conventional RAS recirculate up to 98% of the water within the system, which is roughly 1,000 litres of fresh water per kilogram of feed added. For reference, flow-through systems have an exchange rate greater than 50,000 litres of water per kilogram of feed. The only reason it is feasible to treat the waste stream in a RAS is because it is low flow and high concentration compared to a flow-through system. Flow-through systems can have an effluent stream that is 10 to 100 times larger and 10 to 100

times more dilute than that of a RAS. Furthermore, the make-up water added to the RAS must be clean to avoid introducing foreign compounds and pathogens into the system and for this reason groundwater is preferred over surface water.

1.3 Cooke Aquaculture Partnership

Cooke Aquaculture Inc. is a Canadian company with operations in nine countries and is a prominent partner for recirculating aquaculture research at the University of New Brunswick. Although Cooke Aquaculture farms 17 different species of fish, the bulk of its operation is in the farming of *Salmo salar* (Atlantic salmon). Salmon are currently grown in land-based freshwater RAS until the smolt stage (80 to 100 grams) and are then transported to sea cages to grow until they are harvested at four to five kilograms after 16 to 18 months (Waycott, 2019). An exception is broodstock, which are not sent to sea cages and spend their entire life in a freshwater RAS. Broodstock are used for breeding and can grow upwards of 20 kg after multiple years. In New Brunswick, all of Cooke Aquaculture's Broodstock are raised and kept at Oak Bay Hatchery in Oak Bay.

In sea cages, salmon are exposed to natural diseases and may escape, if storms cause damage to equipment. Consequently, the less time the salmon spend in sea cages, the less risk is involved for the farmers. This is creating an incentive for salmon to be raised to a post-smolt stage within RAS. However, with farm outputs growing larger both in the number and size of the salmon, the waste-solids produced are increasing as well, thus the push for better solids disposal. In Johnson Lake, New Brunswick, Cooke Aquaculture is currently constructing their largest land-based farm for the production of salmon parr,

which will be operational in May 2023. The Johnson Lake Hatchery will have a feed loading rate of 2,000 kilograms per day during peak production.

1.4 Waste-Solids

Gravity settling units such as swirl separators and radial flow separators are commonly used for waste-solids removal because they are effective at removing large particles and take up little floor space. Shown in Figure 1-2, the water enters the swirl separator by the side which causes a circular flow. The centrifugal force from this current pushes the solids towards the outer walls while the water exits through by overflowing into a pipe located at the centre of the unit. Gravity pulls the solids to the bottom of the unit where they settle until flushed. Radial flow separators follow a similar premise however they have some distinct differences. Shown in Figure 1-3, the water enters the radial flow separator from the centre and is propelled upwards into a shroud. The water then flows radially under the shroud and towards the outer radius of the unit while gravity pulls the solid particles towards the bottom where they settle until flushed. Depending on the design of the unit, the water can exit by flowing over a weir located around the outer radius of the unit or by overflowing into a pipe located outside of the shroud. Swirl separator and radial flow separators do not have a high efficiency for removing microparticles and are most often followed by a drum filter. Drum filters are the preferred method for removing microparticles due to their low head and being easy to operate. Once removed from the system water, the solids are sent to a septic tank where they are held until being disposed of (Timmons, Ebeling, Wheaton, Summerfelt, & Vinci, 2001).

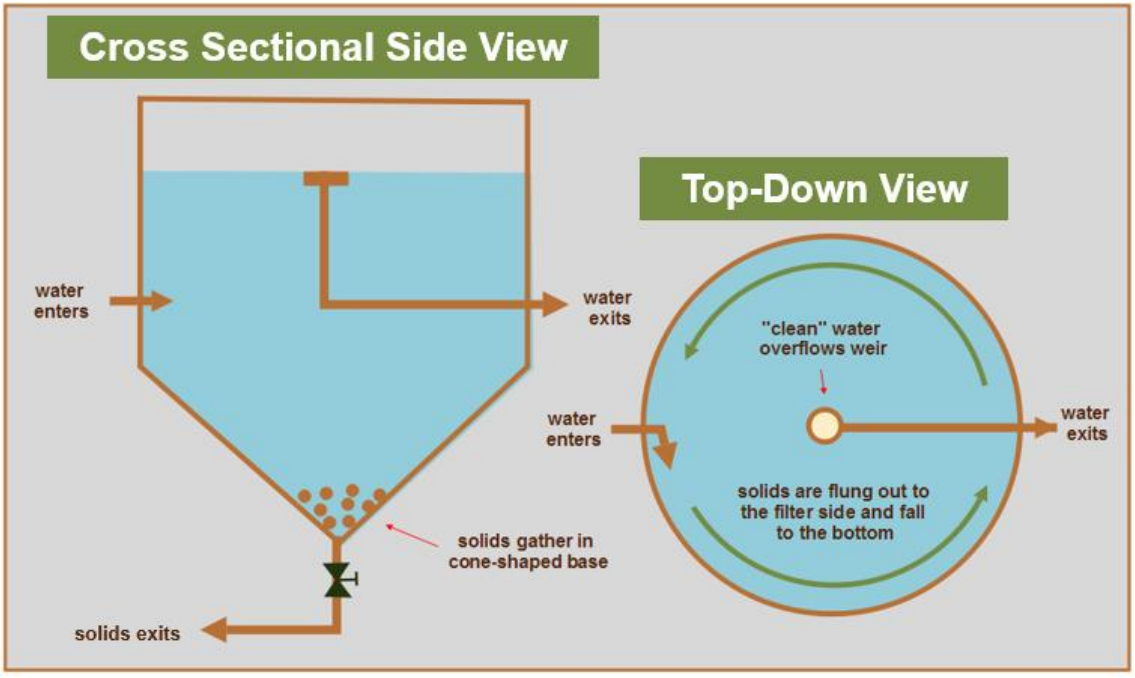

Figure 1-2: Schematic of a swirl separator. Image modified from (Donaldson, 2017).

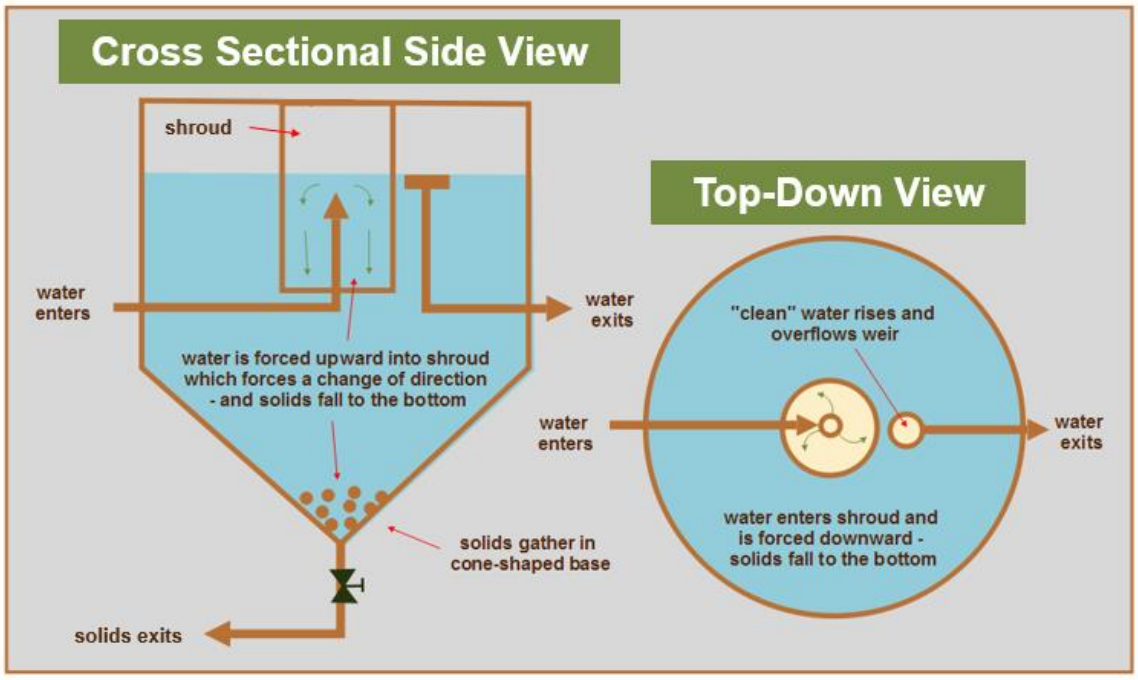

Figure 1-3: Schematic of a radial flow separator which water exits by a pipe outside of the shroud. Image modified from (Donaldson, 2017)

Improving the management of solid waste produced in a RAS has an environmental and an economical benefit. Most solid waste produced in a RAS is used as a fertilizer, sent to landfills, used for vermiculture, or treated in municipal waste facilities (Cripps & Bergheim, 2000) (Martins, et al., 2010) (Timmons, Ebeling, Wheaton, Summerfelt, & Vinci, 2001). Regardless of what is done with the waste solids, they must be transported off-site. Cooke Aquaculture pays approximately $150 per tonne of sludge to move the sludge from the land-based farm to the disposal location. This cost consists of transportation, storage, labour, and disposal fees, all of which can be reduced by dewatering the waste, decreasing its volume and weight (Timmons, Ebeling, Wheaton, Summerfelt, & Vinci, 2001). At the height of the production cycle at Johnson Lake Hatchery, 30 tonnes per day of waste at 2 wt.% solids initially will be produced. Dewatering this waste to 25 wt.% solids would result in only 2.4 tonnes per day of waste being produced at peak loading and a 92% weight reduction. The percent weight reduction from other initial weight percentages can be determined by Figure 1-4.

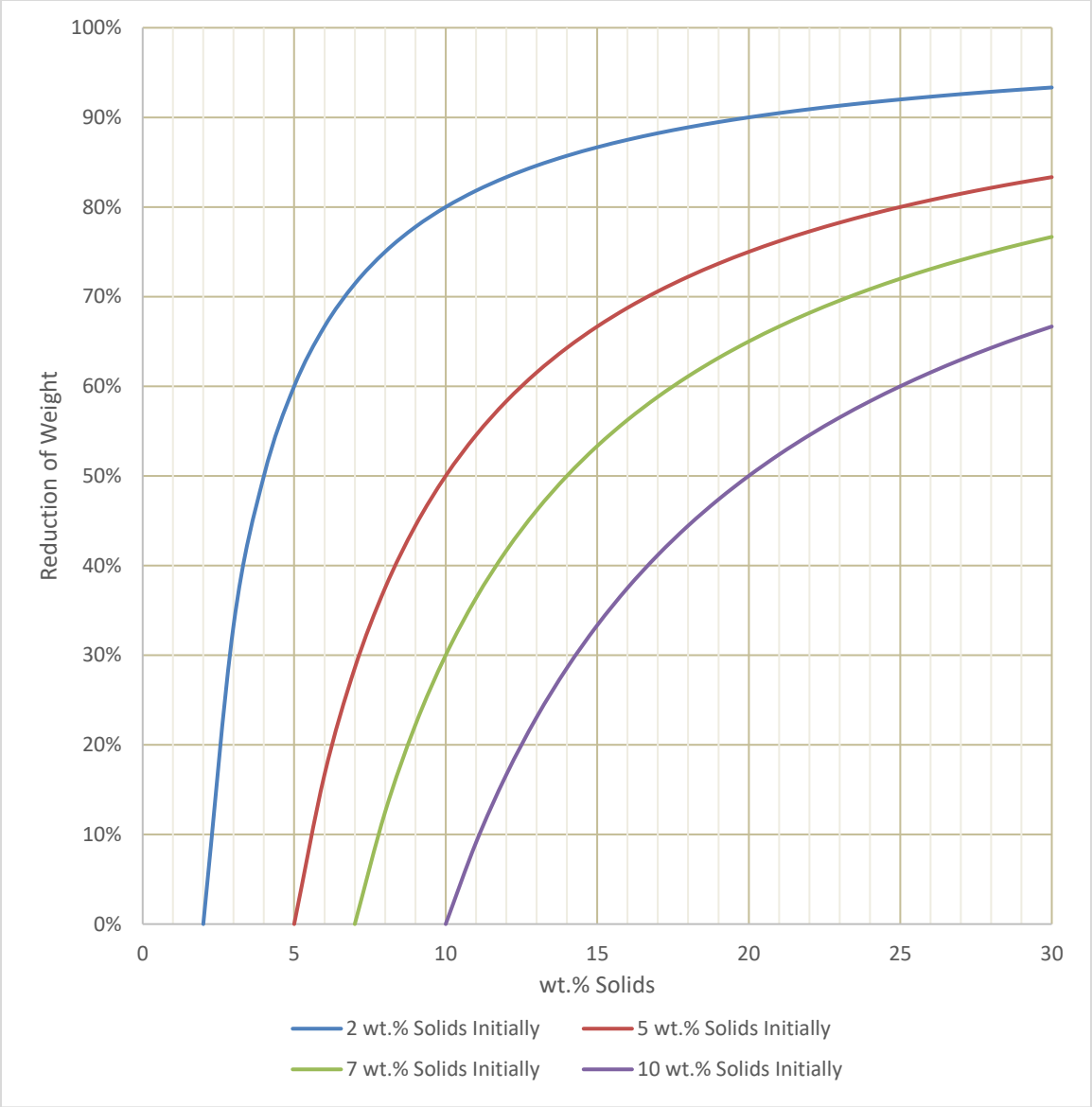

Figure 1-4: Water weight reduction by dewatering sludge.

Removing water from the sludge would reduce its weight and correspondingly reduce cost of transporting it offsite for disposal. Aquaculture currently lacks an efficient and effective method to dewater sludge prior to offsite disposal. No research data exists for centrifuges and the viability of using centrifugation to remove water from aquaculture sludge should be investigated.

1.5 Objectives

The goal of this research was to determine the ability of a centrifuge to dewater aquaculture sludge. To achieve this goal, the research was split into three objectives which consisted of tests with a lab-scale centrifuge, tests with a pilot-scale centrifuge and the investigation of incineration as an onsite disposal method. The objectives were the following:

a. To evaluate different physical and chemical conditioners and optimize dosing levels using a lab-scale centrifuge.
b. To use a pilot-scale basket centrifuge and the optimal conditioner dosing found in the previous sub-objective to determine the cake dryness that can be achieved.
c. To determine whether waste-solids that have been dried by centrifugation are dry enough to be incinerated.

Chapter 2: Literature Review

2.1 Dewatering Technologies

Current sludge thickening units used in aquaculture such as gravity settlers and drum filters cannot achieve solid concentrations greater than approximately 10 wt.% (Timmons, Ebeling, Wheaton, Summerfelt, & Vinci, 2001) (Sharrer, Rishel, Taylor, Vinci, & Summerfelt, 2010). In order to achieve a higher concentration of solids, new technologies must be explored. Possible technologies that could be used for advanced dewatering of RAS wastes include belt filters, geotextile bags, artificial wetlands, and centrifuges (Sharrer, Rishel, Taylor, Vinci, & Summerfelt, 2010) (Boxman, et al., 2015) (Martins, et al., 2010) (Timmons, Ebeling, Wheaton, Summerfelt, & Vinci, 2001). To determine the feasibility of several of these technologies, Sharrer et al. (2010) compared the dewatering capability to the economic viability. They discovered that inclined filter belts, gravity thickening, and geotextile bags could dewater aquaculture sludge to a final dry solid percent of 11 wt.%, 10 wt.%, and 21 wt.%, respectively. Although the geotextile bag achieved high dewatering, it was also the least economic option with an estimated capital cost of $612,000 USD and a yearly cost of $120,000 USD for the fabric in a 454 tonnes per year facility. The geotextile bag excelled at solids removal; however, due to leaching, the water leaving the bag was highly contaminated with nutrients. Boxman, et al. (2015) solved this issue by passing the wastewater through a constructed wetland to remove excess nutrients. This method was exceptional for removing phosphorous and nitrogen, however it greatly increased the land requirement. This study took place in a warm climate, and it should be noted that geotextile bags filters freeze in

sub-zero conditions, rendering them useless during the winter in colder climates. Yeo, et al. (2004) investigated the dewaterability of a filter press and concluded that 35% of water could be removed from aquaculture sludge for a dry solids content of 3%. This was obtained with the use of a physical additive: fly ash, agricultural lime, diatomaceous earth, or pearlite additives.

Centrifuges should be investigated as a possible technology for the dewatering of RAS waste solids. A centrifuge capable of dewatering the solids of the Johnson Lake Hatchery facility from 2 wt.% solids to 20 wt.% solids would have a pay-back period of less than 2 years. Researchers Timmons, et al. (2001) and Wakeman (2007) claim that centrifuges are a viable option for dewatering aquaculture sludge. Centrifuges separate solids and liquids by using centrifugal force. Sludge is continuously pumped into the spinning centrifuge bowl where it is subjected to a centrifugal force that pushes it against the bowl wall. A helical screw rotates at a slightly slower rate and guides the thickened sludge towards the conical end and the separated water towards the other end (Wakeman, 2007). A cross-sectional side view of a typical decanter centrifuge is depicted in Figure 2-1. A key innovation in newer centrifuge designs is a gate to adjust the thickness of the sludge cake formed on the walls. This gate scrapes off the wetter top layer of sludge and only allows the driest cake layer to exit the centrifuge. The wetter top layer is then recycled back for further dewatering (Wakeman, 2007).

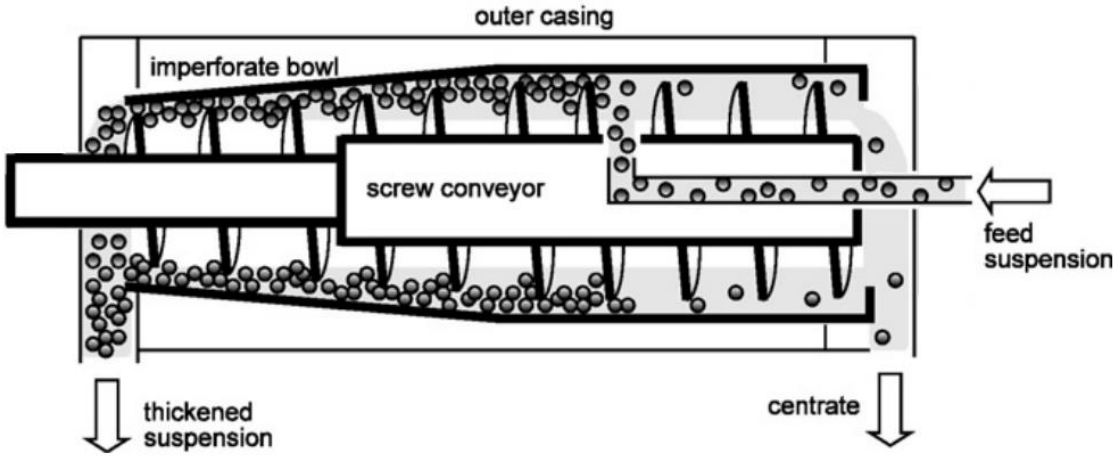

Figure 2-1: Cross-sectional view of a decanter centrifuge (Wakeman, 2007).

Centrifuges have been used for wastewater treatment in many industries and it is frequently used for dewatering municipal activated sludge (Davis, 2010) (Wakeman, 2007). Centrifuges are used to achieve a very high solids content in municipal sludge, reaching consistently between 20 wt.% to 30 wt.% dry solids (Wakeman, 2007). This is notably higher than the dryness that can be achieved with conventional aquaculture equipment, where the only system capable of producing 20 wt.% dry solids is the geotextile bag filter (Sharrer, Rishel, Taylor, Vinci, & Summerfelt, 2010).

The ability of several technologies to dewater aquaculture sludge, primary municipal wastewater sludge, and waste activated sludge (WAS) is compared in Table 2-1. The solids contents achieved with both aquaculture sludge and WAS are similar, and lower than those for the primary sludge. It is therefore anticipated that centrifuges can provide results for aquaculture sludge similar to those achieved for WAS.

Table 2-1: Comparison of aquaculture sludge to other types of sludge (Sharrer, Rishel, Taylor, Vinci, & Summerfelt, 2010) (Yeo, Binkowski, & Morris, 2004) (Wakeman, 2007).

	Sludge Type (wt.% Solid)		
Technology	**Aquaculture**	**Primary**	**WAS**
Gravity Settler	9	10-15	5-10
Inclined Belt Filter	11	30	15
Geotextile Bag Filter	22	45	15
Filter Press	3	28-44	25-35
Centrifuge		25-40	16-25

2.2 Classification of Water in Sludge

The dewaterability of a sludge is dependent on the physical water distribution within the sludge. As depicted by Figure 2-2, there are four types of water within a sludge: free, interstitial, surface, and intracellular water. Free water has no physical or chemical bond to the solid particles and is the only type which can be completely removed from the sludge using mechanical dewatering techniques (Kopp & Dichtl, 2001) (Wei, Gao, Ren, Li, & Yang, 2018). Interstitial water is water that is caught within the solid structure, and only some interstitial water can be removed by mechanical dewatering techniques (Vesilind, 1994) (Wei, Gao, Ren, Li, & Yang, 2018). Surface water is directly bound to the surface of the solid by hydrogen bounding, is difficult to mechanically remove, and accounts for less than 5% of total water (Judd, 2020). Intracellular water is found within the cells of bacteria in the sludge. This water is difficult to remove mechanically as the cell wall must be ruptured to release this trapped water (Liu, et al., 2018).

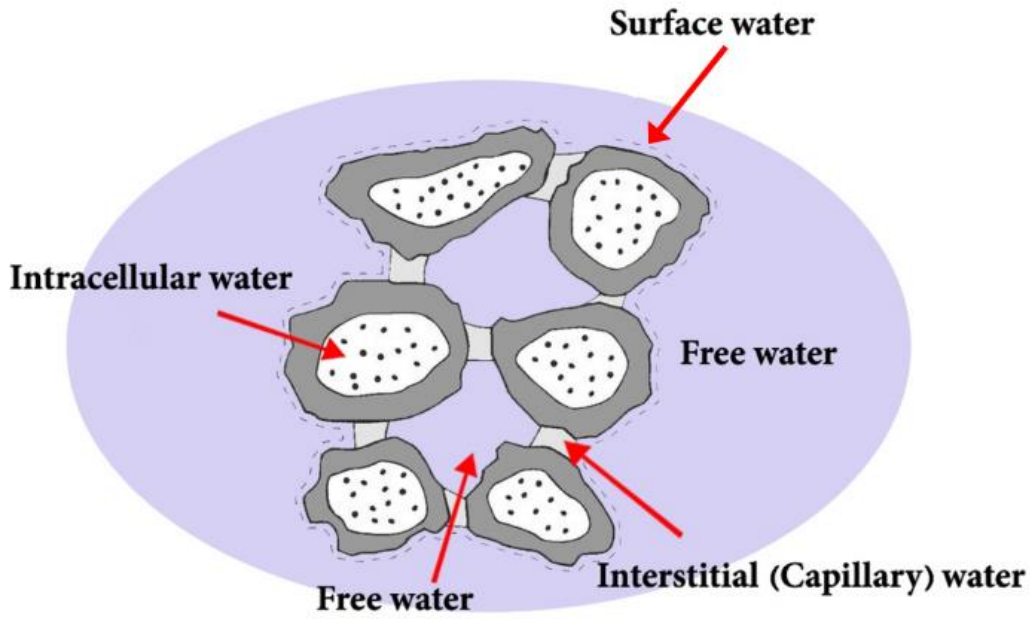

Figure 2-2: Types of water within sludge (Kootenaei, et al., 2022).

2.3 Chemical Conditioners

Typically, chemical conditioners are added prior to the dewatering unit. Coagulation and flocculation are commonly used in wastewater treatment and in many other industries such as mining, oil extraction, and paper pulping to facilitate liquid-solid separation (de Milieux, 2014) (Wei, Gao, Ren, Li, & Yang, 2018). A sludge is a colloid which consists of organic suspended solids. These particles have a negative surface charge which cause them to repel and remain suspended in the solution. The purpose of the coagulant is to coat the particles and neutralize their negative charge in order for the particles to aggregate and settle. Trivalent metal ions are commonly used as coagulants due to the high charge neutralization they offer. The neutralization of the particles can also reduce the thickness of the hydrated shell of the particles and further increase the free water

content of the sludge. Flocculants are polymers that sweep through the solution connecting the aggregated particles, creating large flocs, and speeding up the settling process. This mechanism is known as bridging (Wei, Gao, Ren, Li, & Yang, 2018). Flexible, long chain organic polymers are commonly used as flocculants. A high molecular weight facilitates bridging, and some flocculants weigh more than 10,000,000 grams per mole. Sludge flocs that have been formed by high molecular weight polymers increase the sludge's structure and hence increase the dewaterability (Wei, Gao, Ren, Li, & Yang, 2018).

Water leaves the sludge through interstices called pores and larger pores allow the water to leave faster. When small solids settle, they form a compact bed with very narrow pores causing a slow release of water. When the large solids floc together, they create a less compact bed with larger interstices, resulting in a quicker release of water (Gray, 2015) (de Milieux, 2014). This effect is shown in Figure 2-3.

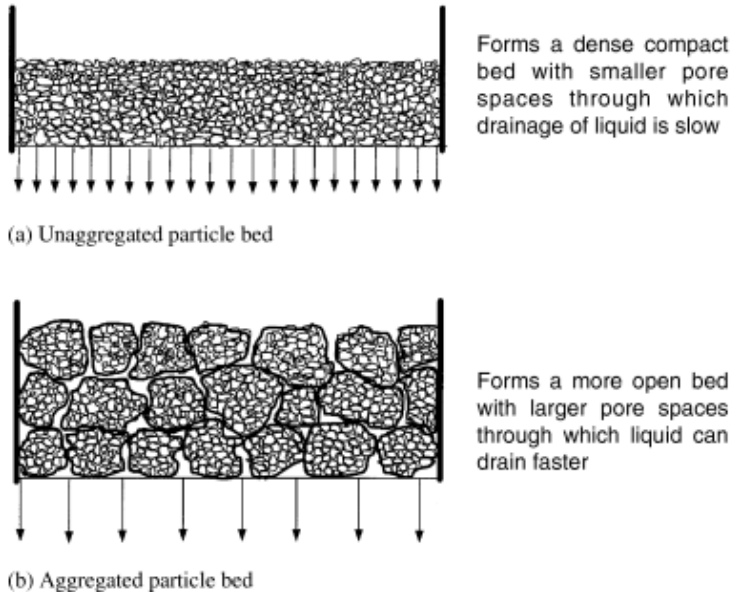

Figure 2-3: Larger flocs create larger interstices (Gray, 2015).

In terms of dosage, an insufficient amount of coagulant and flocculant results in poor aggregation and bridging, however an overdose also exists. An overdose of coagulants can regenerate the suspension ability of the particles. This is called the restabilization effect and is due to the superabundance of positive charge in the solution. Consequently, this also increases the turbidity. Flocculants initially increase the dewaterability of the sludge, but an optimal amount is quickly reached. The increase in viscosity caused by the addition of the heavy polymer will eventually compromise the dewaterability of the sludge (Wei, Gao, Ren, Li, & Yang, 2018).

2.4 Physical Conditioners

As the pressure increases, chemical conditioning starts to become less effective at dewatering sludge (Zhang, et al., 2019). This is because the pore structure collapses once the pressure exceeds a certain threshold and compresses the sludge, trapping the water deep inside (Wei, Gao, Ren, Li, & Yang, 2018). Physical conditioners can be added to sludge to increase the dewaterability by providing a skeleton structure to the sludge. This reduces the compressibility of the sludge and as seen Figure 2-4, the pores remain open so interstitial water can exit (Zhang, et al., 2019) (Wei, Gao, Ren, Li, & Yang, 2018) (Ding, et al., 2014). Zhang et al. (2019) explained that powdered coal ash, lime, sawdust, gypsum, red mud, lignite, rice husk char are common physical conditioners and determined that woodchips were the most effective for dewatering. Ding, et al. noticed that when tested on a bench-scale, physical conditioners did not impact the dewaterability of sewage sludge. They concluded that physical conditioners offer little to no effect at low pressures. When they used a bench-scale plate-and-frame filter press with chemical

conditioner at a process pressure of 80 kPa, the highest obtained solids content in the sewage sludge was 12.1% and adding woodchips improved dewaterability by an insignificant amount. Meanwhile, when a pilot-scale plate-and-frame filter press was used with physical conditioners at a process pressure of 1 MPa the highest obtained solids content was 50.7% compared to 23.9% without.

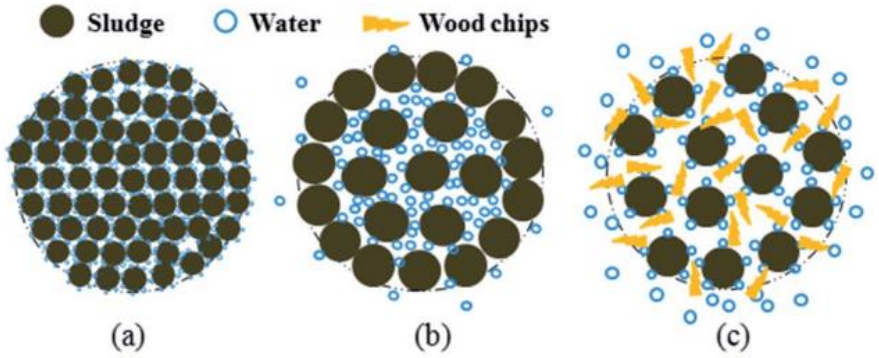

Figure 2-4: (a) sewage sludge with no conditioning, (b) sewage sludge with only chemical conditioning, (c) sewage sludge with chemical and physical conditioning (Ding, et al., 2014).

Chapter 3: Methodology

3.1 Sludge

The sludge used for this experimental study was collected from the Oak Bay Hatchery. Every line at the Oak Bay Hatchery houses different aged fish and sludge was sampled from two different lines and the septic tank. The majority of sludge at Johnson Lake Hatchery, and other hatcheries owned by Cooke, will be produced by young salmon, usually in the parr life stage. As a result, the sludge from juvenile salmon is of most interest. Oak Bay Hatchery does not have any salmon parr and as a result, young broodstock sludge was used due to being the most similar to sludge from parr. Due to being much larger fish, adult broodstock produce a lot of sludge, which is visibly different than sludge from younger fish. For this reason, broodstock sludge was also sampled. The centrifuge at Johnson Lake Hatchery operates in batches that begin once the sludge holding tank is full and ends once it is empty. Depending on feed loading rate, sludge could be sitting in the tank for days before it becomes full. As sludge ages, bacteria digest the fecal matter and after a certain period the sludge becomes mostly bacteria. For this reason, sludge from the septic tank was also sampled.

3.1.1 Young Broodstock Sludge

The first source of sludge was from the swirl separator in D-line. This line exclusively contains young broodstock fish with an average weight of 1.5 kg. The sludge is collected from the top of the layer of settled solids in the swirl separator by scooping it out with a fine mesh net. As seen in Figure 3-1, the sludge is fresh, still in pellet form, and was initially around 8 wt.% solids.

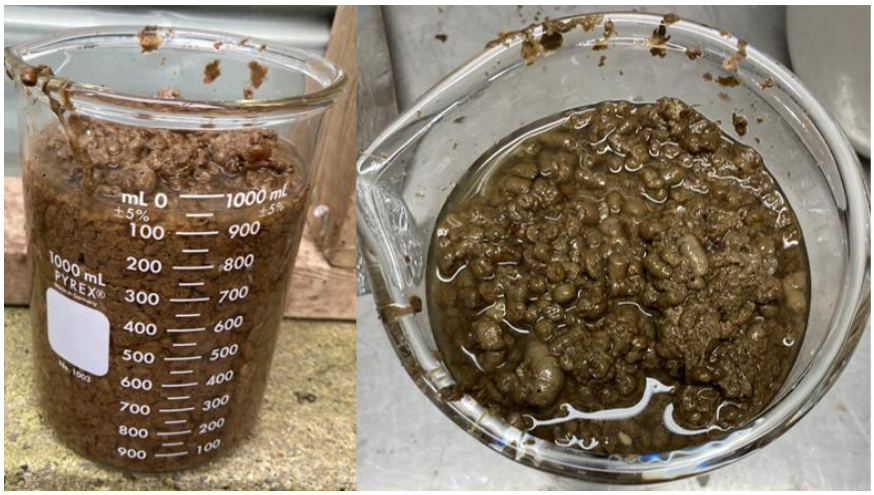

Figure 3-1: Young broodstock sludge from the swirl separator in D-line.

3.1.2 Adult Broodstock Sludge

The second source of sludge was from the radial flow separator in E-line, which contained broodstock fish with an average weight of 15 kg that were being prepared for spawning. The sludge was drained out through the bottom of the radial flow separator and was initially around 7 wt.% solids. As seen in Figure 3-2, the feces in E-line were loose, amorphous, and stringy, as opposed to the pelleted feces found in D-line. According to experienced hatchery personnel, once the salmon reach 2 kg, the feces are no longer excreted as pellets. Both D-line and E-line fish are fed Skretting Optiline RC 500 80A 6mm pellets, which contain an agent to bind up fecal matter to facilitate filtration and settling.

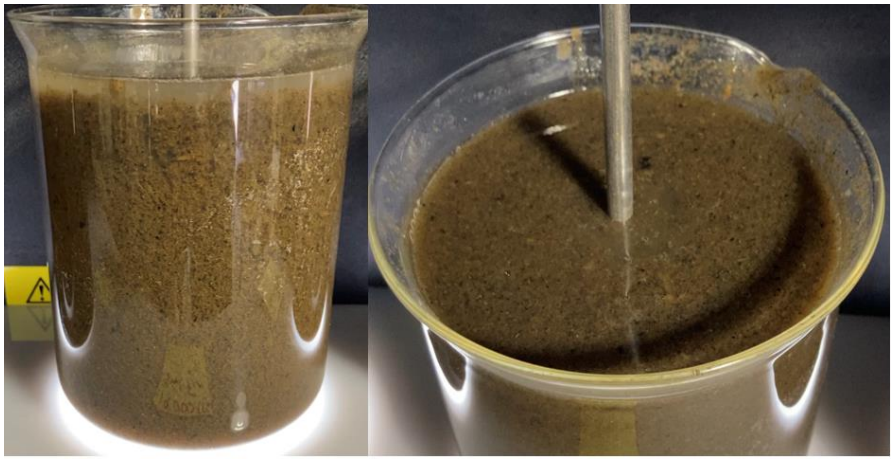

Figure 3-2: Adult broodstock sludge from the radial flow separator sludge in E-line.

3.1.3 Septic Tank Sludge

The final source of sludge was from the septic tank and was collected by lowering a bucket on a pole into the tank. The sludge from all sections of the hatchery is sent to the septic tank and as a result this tank contains feces from all stages of the salmon lifecycle. The septic tank is emptied after several weeks of operation once it is full, which gives plenty of time for the sludge to undergo digestion. Shown in Figure 3-3, the sludge is darker than fresh sludge, has a grainy appearance and was initially 10 wt.% solids.

Figure 3-3: Aged sludge from the septic tank.

3.2 Sludge Drying

The sludge's solid content was determined using a Thermo Scientific Precision model 658 Gravity Convection Oven and scale with an accuracy of ± 1 mg. After recording the sludge sample's weight (m_{sludge}), the sample was placed in the oven at 105°C. After remaining in the oven 15 hours, all the water was evaporated from the sludge sample and only the dried solids remained. Once removed from the oven, the sample was placed in a desiccator so it could cool without absorbing any moisture from the air. Once the sample had cooled to room temperature, the weight of the dry solids (m_{solids}) was recorded, and Equation (3-1) was be used to calculate the samples wt.% solids.

$$wt.\%\ solids = \frac{m_{solids}}{m_{sludge}} \cdot 100\% \quad \textbf{(3-1)}$$

3.3 Chemical Conditioners

In order to help dewatering, chemical and physical conditioners were used. In terms of coagulants, ferric sulfate (FS) and poly-aluminium chloride (PAC) were available for use. In addition, the flocculant polyacrylamide (PAM) was used. Unlike FS and PAC, which are liquids, PAM was received as a powder and had to be dissolved. Although PAM has a high solubility, it tends to form clumps as the long polymer chains become entangled with one another. Before use, the solution was mixed until no large clumps were left in solution. A concentrated 10 g/L solution was used so that only a small amount needed to be added to the sample and thus avoiding increasing the sample's volume.

3.4 Jar Test

The Phipps and Bird jar test was used to determine the optimal dose of chemical conditioners. Shown in Figure 3-4, the jar test is an apparatus that lights up the bottom of beakers while consistently mixing the sludge samples. This allows for multiple samples to be visually compared at once. The mixing speed of the apparatus was adjustable, and the sludge was mixed at 75 rotations per minute (RPM). This speed was selected because it is high enough to enforce good mixing, yet low enough to not shred the flocs. The chemical conditioners are said to be effective if flocs are formed after long mechanical mixing, re-flocculates when broken up, decrease the turbidity of the free water, and most importantly yield the lowest moisture content when spun on the lab-scale centrifuge. The turbidity of the free water was measured using a Hach DR900 colorimeter. Turbidity is caused when a large number of microparticles are in suspension and the clarity of the

liquid is reduced. When effective, chemical conditioners will cause the microparticles to floc together and decrease the turbidity.

Figure 3-4: Various doses of chemical conditioners tested with a jar test.

3.4 Physical Conditioner

The sole physical conditioner tested was sawdust due to it being easy to obtain, relatively inexpensive, and biodegradable. Cedar sawdust was obtained from a local lumber yard and as shown in Figure 3-5, was relatively fine. Sawdust was added in ratios of 1:8, 1:4, 1:2, and 1:1 (grams of dry sawdust: gram of dry sludge). Although the sawdust was dosed by its dry weight, the sawdust was not dried before it was added to the sludge and had a moisture content of approximately 20 wt.% water. If applied on an industrial scale, it is likely that the farms will not possess the equipment to dry the sawdust and for this reason

the sawdust was used as found. It was believed that this addition should reduce the overall compressibility of the sludge by helping it retain structure under the centrifugal force, resulting in a more stable pore structure. This would in turn allow interstitial water trapped in the sludge to drain out along the pores created by the sawdust.

Figure 3-5: Cedar sawdust with a ruler for scale (numbered lines are in cm).

3.5 Centrifuges

Shown in Equation (3-2), centrifugal force is a function of rotational speed and radius, so as a result RPM cannot be used to compare two different centrifuges. Instead, relative centrifugal force (RCF) is used to compare different centrifuges and as seen in Equation (3-3) is the ratio of the centrifugal force and the earth's gravitational force.

$$F_C = m\left(\frac{2\pi(rpm)}{60}\right)^2 r \quad \textbf{(3-2)}$$

$$RCF = \frac{\left(\frac{2\pi(rpm)}{60}\right)^2 r}{g} \quad \textbf{(3-3)}$$

3.5.1 Lab-Scale Centrifuge

The lab-scale centrifuge used to determine the optimal dosage was an Eppendorf 5804 centrifuge equipped with a swinging bucket rotor and can be seen in Figure 3-6. This is a batch centrifuge which can hold sixteen 50 mL standard conical centrifuge tubes and can operate at a max speed of 4,200 RPM, or a RCF of 3,234-G.

Figure 3-6: Eppendorf 5804 lab-scale centrifuge equipped with a swinging bucket rotor (Eppendorf, 2023).

3.5.2 Pilot-Scale Centrifuge

The pilot-scale centrifuge used was a US Centrifuge Systems M512 centrifuge. This centrifuge is a basket centrifuge that operates as a semi-continuous batch which means that the sludge is continuously fed into the bowl and the supernatant continuously exits through the top of the bowl while the solids accumulate in the bowl. A cross-section of the M512 can be seen below in Figure 3-7. Once the bowl is full of solids, the unit is left to spin for an additional 5 mins before the cycle is ended. It is suggested that the unit is run until approximately 1 US gal of solids has accumulated in the 1.6 US gal bowl, however for dewatering purposes it was determined to work best if the unit is run until the bowl is completely full. This unit was fed at roughly 1 US gpm and has one operating speed of 3,000 RPM, or 1,500-G.

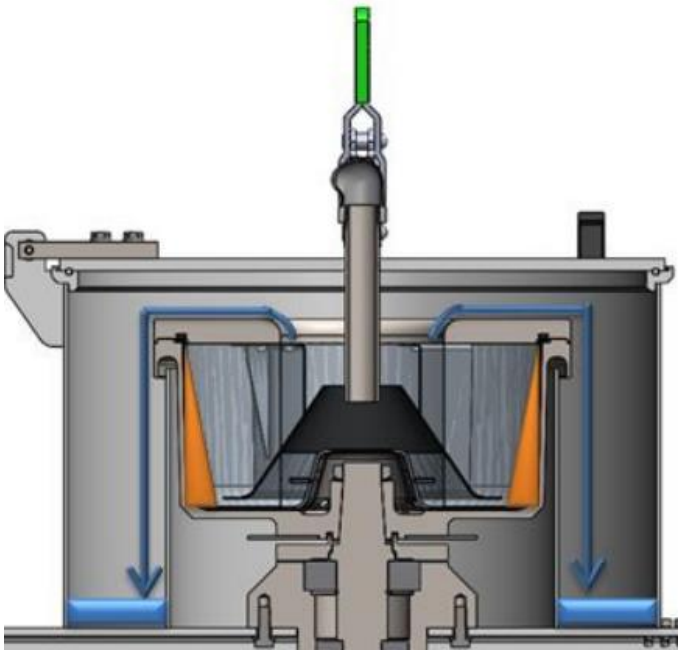

Figure 3-7: Cross sectional view of an M512 basket centrifuge (US Centrifuge Systems, 2014).

3.6 Bomb Calorimeter

The calorific value, or higher heating value (HHV), of sludge was determined using a Parr Instrument Company oxygen bomb calorimeter. Due to the well-insulated container surrounding the bomb calorimeter system seen in Figure 3-8, the heat gained by the system is equivalent to the heat given off by the combustion of the sample and the ignition wire. This is demonstrated by Equation (3-4) and can be expanded into Equation (3-5). By measuring the change of temperature of the water in the system, Equation (3-5) can be used to determine the HHV of the sludge sample. The energy released from the ignition wire (H_{Wire}) used was 0.0481 kJ/cm and the length ignited (L_{wire}) was obtained by measuring the wire before ignition and the remaining wire after ignition. To standardize the bomb calorimeter, the first three trials were run with 1 g pellets of benzoic acid. This is done to get the energy equivalent (E_{System}) of the system by using Equation 3.1. Benzoic acid is used for standardization because it has a well recorded HHV of 26.43 kJ/g and is easily obtainable in a 99.9% pure form. It was determined that the specific bomb calorimeter used for these trials had an energy equivalent of 10.37 ± 0.16 kJ/°C.

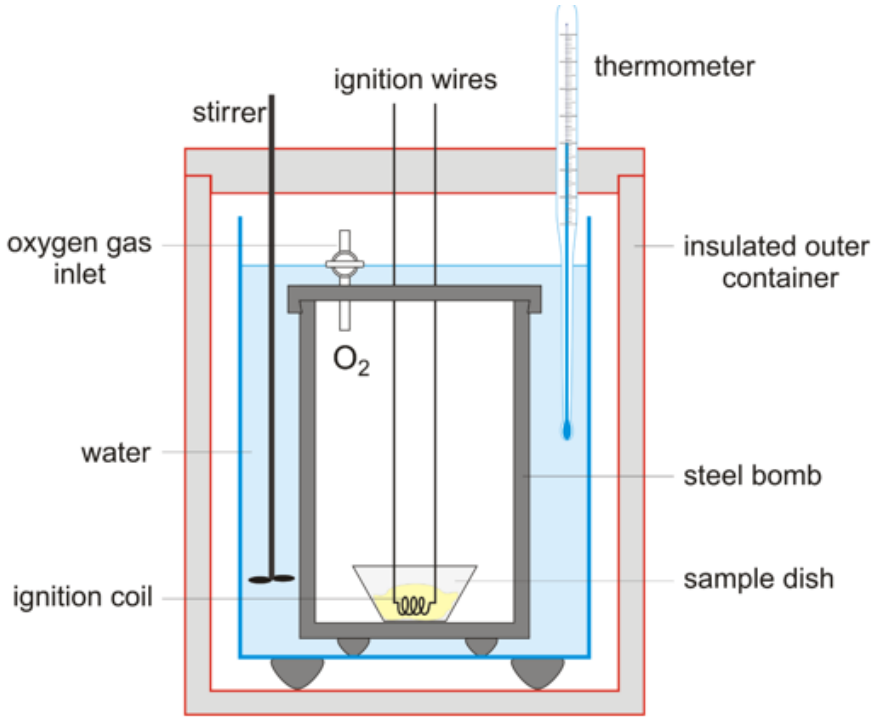

Figure 3-8: Components of an oxygen bomb calorimeter (Generalic, 2022).

$$Q_{System} = -(Q_{Sample} + Q_{Wire}) \quad \textbf{(3-4)}$$

$$E_{System} \cdot \Delta T = -(HHV \cdot m_{Sample} + H_{Wire} \cdot L) \quad \textbf{(3-5)}$$

Dried sludge samples were ground to a fine powder using a pestle and mortar before being pressed into 1g pellets using a pellet press. After being weighed to mg accuracy, the pellets were placed on the sample dish and sealed within the metal bomb. The metal bomb was filled with 20 atm (2026.5 kPa) of pure oxygen, then purged to remove any nitrogen from the air in the bomb and refilled back to 30 atm for a true pure oxygen environment. The bomb was then submerged in 2.000 kg of room temperature (20 °C) deionized water and placed in the insulated container. The sample within the bomb was

then ignited using an electrical current through the ignition wire and the change in temperature of the system was recorded to an accuracy ± 0.01 °C.

3.7 Elemental Analysis

For sludge composition, carbon, hydrogen, nitrogen, and sulfur (CHNS) content was determined by the personnel of the Limerick Pulp and Paper Research Centre using a Perking Elmer PE 2400 CHNS Elemental Analyzer. The trace metal concentration was determined by the personnel of the Research and Productivity Council using inductively coupled plasma mass spectrometry. The fixed solids, or ash, was found by measuring the remaining mass after burning off the volatile solids in a furnace. With a temperature profile of 3 °C/min, the solids were brought to 550°C and held at that temperature for one hour to burn off all the volatile solids. Prior to all three tests, the samples were dried in the oven at 105°C and ground using a pestle and mortar.

Phosphorous concentration in the supernatant was determined using a Lamotte SmartSpectro spectrophotometer and the Lamotte phosphate high range test (Code 3655 SC). The concentration was then verified by diluting the same sample and using Hach DR900 colorimeter and the Hach Method 10209, which is a low range test. Prior to testing, any potential solids were removed by vacuum filtration using 1.6 μm particle retention glass fiber filters.

3.8 Particle Density

As done by Patterson and Watts in 2001, the sludge particles were submerged in multiple sucrose solutions of varying concentration to determine their density. As the sucrose concentration increases, so does the density of the solution which increases the buoyant

force on the particles (Heidcamp, 2017). If the particles float, it can be said that their density is less than that of the solution and in the contrary, the particle will sink if it is denser than the solution. The approximate particle density can be determined by finding the sucrose concentration at which the particles change from floating to sinking. To create the solution, sugar was dried in the oven at 105°C to remove moisture before it was weighed and added to distilled water. To verify the density, 10.0 mL of the solution was added to a 10 mL volumetric flask using a burette and weighed.

For dried sludge particles, the density was determined by weighing a sample and then finding its volume using liquid displacement. A sample of dried solids was weighed and added to a 10 mL volumetric flask. Using too little of a sample will result in a small volume which can increase the experimental error. Dried sludge is hydrophobic and as a result water cannot fully penetrate the layer of solids as the flask is being filled. To overcome this issue, isopropyl alcohol (IPA) was used instead of water. The amount of IPA required to fill the flask was recorded using a burette and by knowing that the volume of the flask is 10 mL, the volume of the solids can be calculated. The particles' mass and volume can then be used to determine their density.

3.9 Particle Size

Particle size analysis was done by taking a picture of sludge under a microscope and using ImageJ software. The microscope used was a Boreal stereomicroscope and to photograph the sludge, a smartphone was placed in a digiscoping adapter that was mounted to one of the eyepieces. Additionally, the microscope was equipped with a frosted glass stage plate and an in-base illuminator. ImageJ identifies particles by their

colour contrast against the background, and this configuration yielded the clearest contrast. Additionally, the colour was edited out of the images to increase the contrast between the white background and the brown particles.

The sludge was placed on a glass calibration slide and water was dropped onto the slide using an eye dropper to dilute the sample and separate the particles from one another. The calibration slide had a 200 µm diameter circle and by using it as a reference point, the software is able to create a scale for the image in µm/pixel. The software then identifies the particles, labels them, and creates an outline. Using the scale, the software then counts the pixels within the particle outline and calculates the projected area of each particle. The ImageJ analysis process is shown below in Figure 3-9.

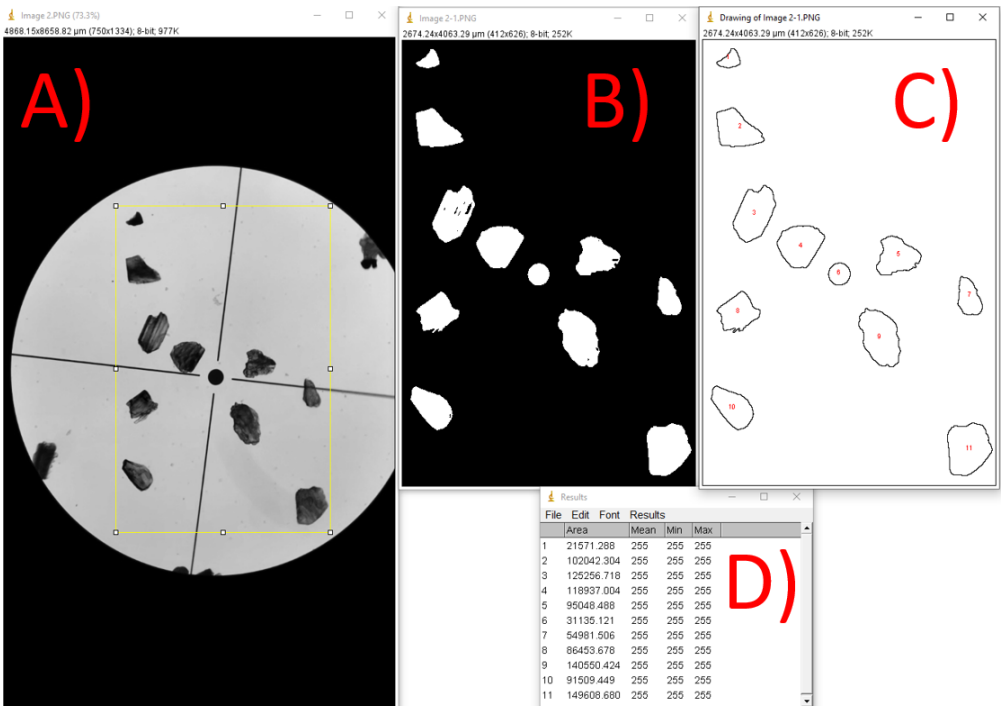

Figure 3-9: A) Sludge is photographed and the area of analysis is selected (reference circle: Ø = 200 µm). B) The particles are identified. C) The particles are outlined and labeled. D) The projected area of each particle is calculated.

Although most particles were not spherical, it was assumed that they were in order to get an approximation of their diameter. Under this assumption, the particle's diameter can be calculated using projected area determined by ImageJ and the formula for the area of a circle.

Chapter 4: Mathematical Models

4.1 Basket Centrifuge Capture Efficiency

The capture efficiency of a centrifuge is commonly modeled assuming the flow in the centrifuge is laminar, however experimental data has shown that this model is often an overestimation of what can be attained in practice (Svarovsky, 2000). For this reason, the capture efficiency was also modeled under fully turbulent conditions. By using both models as extremes, the actual capture efficiency is bound between the two.

4.1.1 Laminar flow

A basket centrifuge can be modeled as a tubular centrifuge and the model used for a tubular centrifuge's efficiency is from the book Solid-Liquid Separation (Svarovsky, 2000). It assumes the following:

- Stoke's Law is valid
- Spherical particles
- Uniform liquid velocity profile (plug flow)
- No mixing (laminar liquid flow)
- Homogenous distribution of particles
- No particles interaction (unhindered settling)
- Inertial forces are negligiable
- No slip condition between the particles and the liquid flow in the axial direction

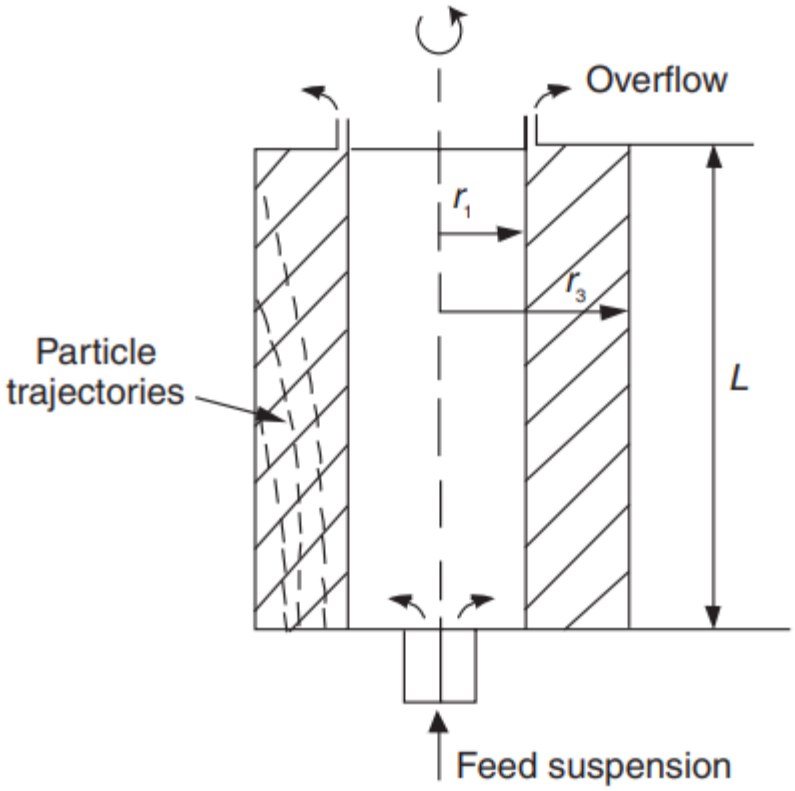

Figure 4-1: Labeled diagram for a tubular centrifuge (Svarovsky, 2000).

Equation (4-1) below is the sedimentation constant (K). It is derived from a modified version of Stokes' law for falling bodies and based off the solid-liquid density difference ($\Delta\rho$), angular velocity (ω), and liquid viscosity (μ). Equation (4-2) is the centrifuge geometry and flowrate constant (K_2) and is equal to the residence time of the liquid. Both constants are used in the particle capture efficiency formula shown in Equation (4-3) (Svarovsky, 2000). It is based off the length of the centrifuge (L), radius from the axis of rotation to the overflow weir (r_1), outer radius of the bowl (r_3), and flowrate (q) (Svarovsky, 2000).

$$K = \frac{\Delta\rho\omega^2}{18\mu} \qquad \textbf{(4-1)}$$

$$K_2 = \frac{L\pi\left(r_3^2 - r_1^2\right)}{q} = \frac{V}{q} \quad \textbf{(4-2)}$$

$$\eta\left(d_p\right) = \frac{r_3^2}{r_3^2 - r_1^2}\left[1 - \exp\left(-2KK_2 d_p^2\right)\right] \quad \textbf{(4-3)}$$

4.1.2 Turbulent Flow

The model was derived under the following assumptions:

- No particle entrainment
- Complete mixing in the radial direction within the liquid layer (turbulent flow)
- Mixing in the longitudinal direction is neglected
- Sedimentation occurs within a thin laminar boundary layer next to the surface of the collected solids
- Particles fall through the boundary layer at their terminal settling velocity
- Unhindered settling
- Plug flow

The capture efficiency of the basket centrifuge, shown in Figure 4-2, for a particle of diameter "d_p" can be obtained as follows. As a result of perfect radial mixing, the concentration of particles (C) above the laminar boundary layer is uniform in any cross-section perpendicular to the flow. However, once the particles reach the boundary layer, they settle at terminal settling velocity (u_t). From this, a mass balance on the particle within the differential element of size "Δh" gives Equation (4-4) which can be simplified using Equations (4-5) and (4-6) to yield Equation (4-7).

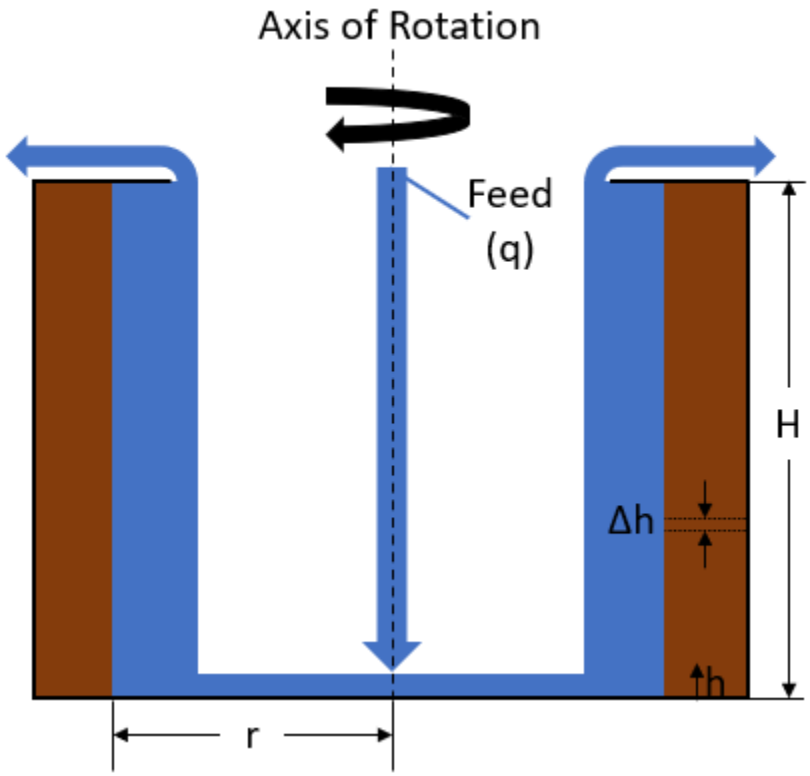

Figure 4-2: Diagram of a basket centrifuge.

$$qC_h - qC_{h+\Delta h} = 2\pi r \Delta h u_t C \quad \textbf{(4-4)}$$

$$C_{h+\Delta h} - C_h = \Delta C = dC \quad \textbf{(4-5)}$$

$$\Delta h = dh \quad \textbf{(4-6)}$$

$$\frac{dC}{dh} = -\frac{2\pi r u_t C}{q} \quad \textbf{(4-7)}$$

Integration of Equation (4-7) over the full length of the centrifuge (*H*) yields (4-8) which simplifies into Equation (4-9). The left-hand side of Equation (4-9) is the natural logarithm of the initial concentration (C_i) and final concentration (C_f). Rearranging Equation (4-9) into exponential form yields Equation (4-10) which can be used to solve for C_f.

$$\int_{C_i}^{C_f} \frac{dC}{C} = -\frac{2\pi r u_t C}{q} \int_0^H dh \quad \textbf{(4-8)}$$

$$\ln\left(\frac{C_f}{C_i}\right) = -\frac{2\pi r u_t H}{q} \quad \textbf{(4-9)}$$

$$C_f = C_i \exp\left(-\frac{2\pi r u_t H}{q}\right) \quad \textbf{(4-10)}$$

The capture efficiency for a centrifuge is shown in Equation (4-11), and is based off the initial concentration and the final exit concentration. Substituting Equation (4-10) into Equation (4-11) results in Equation (4-12). Now the capture efficiency is no longer in terms of concentration and is a function of settling velocity, which is dependent on particle diameter.

$$\eta = \frac{C_f - C_i}{C_f} = 1 - \frac{C_f}{C_i} \quad \textbf{(4-11)}$$

$$\eta(u_t) = 1 - \exp\left(-\frac{2\pi r u_t H}{q}\right) \quad \textbf{(4-12)}$$

4.1.3.1 Settling Velocity

The settling velocity of a particle of any diameter "d_p" within the thin laminar layer can be obtained by writing a force balance in the radial direction on the particle. This force balance includes the external force (F_e), buoyant force (F_b), and drag force (F_D). It is shown in Equation (4-13) and can be expanded into Equation (4-14).

$$m\frac{du}{dt} = F_e - F_b - F_D \quad \textbf{(4-13)}$$

$$m\frac{du}{dt} = ma_e - \frac{m\rho a_e}{\rho_p} - \frac{C_D u^2 \rho A_p}{2} \quad \textbf{(4-14)}$$

Under normal settling conditions, the external acceleration (a_e) is gravity, however in a centrifuge it is proportional to the radius (r) and the angular velocity squared (ω) as shown in Equation (4-15). The terminal settling velocity (u_t) occurs when the rate of

change of the particle's velocity $\left({du}/{dt}\right)$ equals zero and therefore, Equation (4-14) can be rearranged to Equation (4-16) in order to solve for the terminal settling velocity.

$$a_e = \omega^2 r \tag{4-15}$$

$$u_t = \omega\sqrt{\frac{2r\Delta\rho m}{A_p\rho_p C_D\rho}} \tag{4-16}$$

Equation (4-16) can be further simplified using Equations (4-17) and (4-18) for the particle's mass (m) and cross-sectional area (A_p), respectively. This results in Equation (4-19) which is a simplified formula for a spherical particle's settling velocity in a centrifuge based off a force balance.

$$m = \rho_p \cdot \frac{1}{6}\pi d_p^3 \tag{4-17}$$

$$A_p = \frac{1}{4}\pi d_p^2 \tag{4-18}$$

$$u_t = \omega\sqrt{\frac{4r\Delta\rho d_p}{3C_D\rho}} \tag{4-19}$$

The drag coefficient (C_D) for a spherical particle can be obtained using Equation (4-20) which is fitted from data, and shown in Figure 4-3. This data is for spherical particles and is used as an approximation for the particle's C_D. The Reynolds number (Re) for a particle in fluid can be determined from Equation (4-21). The terminal settling velocity required for the capture efficiency can be found by simultaneously solving Equations (4-19), (4-20), and (4-21) for the required particle diameter.

$$C_D = \frac{24}{Re} + 0.22\left(1 + \sqrt{\frac{218}{Re} + 1}\right) \tag{4-20}$$

$$Re = \frac{u_t d_p \rho}{\mu} \tag{4-21}$$

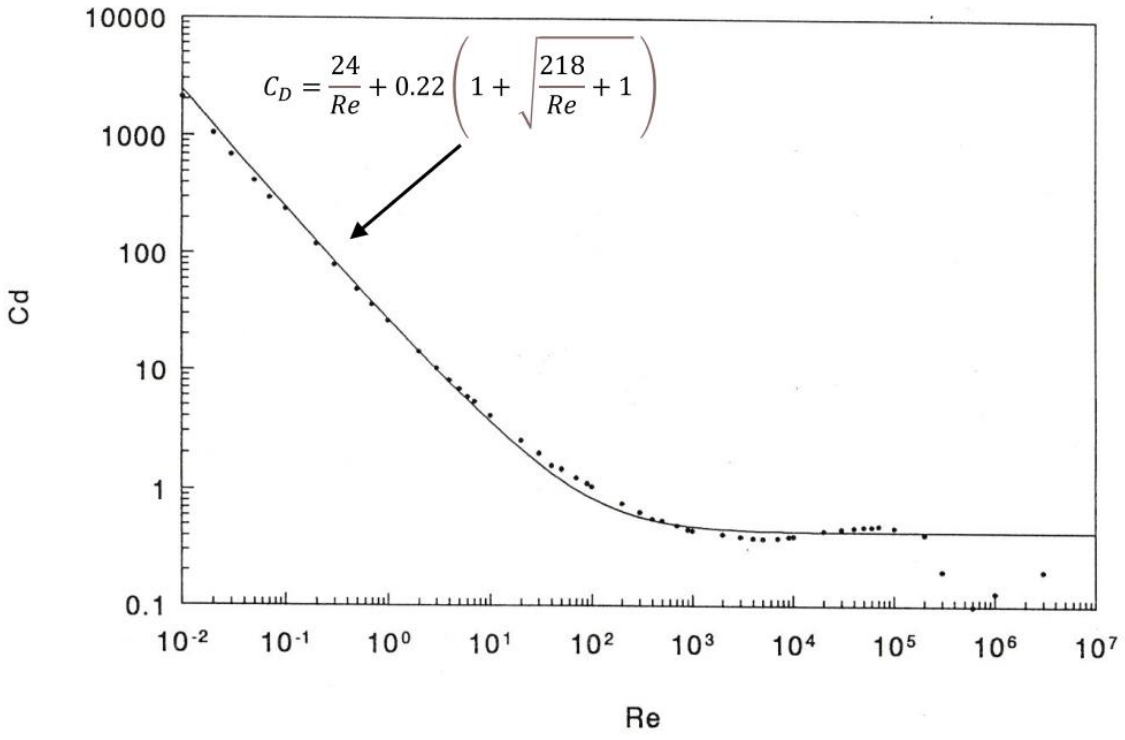

Figure 4-3: Drag coefficient for spheres based off of Reynold number. Data fitted from (Lapple & Shepherd, 1940).

If the particle's Re is less than 1, the settling can be classified as being in the Stoke's region where the formula for C_D is Equation (4-22). By combining Equations (4-19), (4-21) and (4-22), u_t can now be expressed by Equation (4-23). Similar to the laminar model, $\Delta\rho$, ω, and μ can be combined to form the sedimentation constant shown in Equation (4-24). The capture efficiency in the Stoke's region for a case with complete mixing can now be expressed as Equation (4-25) through the combination of Equations (4-12), (4-23), and (4-24).

$$C_D = \frac{24}{Re} \quad \textbf{(4-22)}$$

$$u_t = \frac{\omega^2 r \Delta\rho d_p^2}{18\mu} \quad \textbf{(4-23)}$$

$$K = \frac{\omega^2 \Delta\rho}{18\mu} \quad \textbf{(4-24)}$$

$$\eta(d_p) = 1 - \exp\left(\frac{-2r^2 K d_p^2 H}{q}\right) \quad \textbf{(4-25)}$$

4.2 Adiabatic Flame Temperature Model

The model to predict adiabatic flame temperature in an incinerator assumes the following:

- Complete combustion
- Incinerator is well insulated
- All ash leaves the incinerator with the flue gas as fly-ash
- Humidity in air is negligible
- Air and sludge are at initially 20°C

For an open system such as an incinerator seen below in Figure 4-4, the rate of accumulation of energy within the system $\left({}^{dE}/_{dt}\right)$ is equal to the energy entering the system minus energy leaving the system plus the work done on the system (*W*) and the heat gained by the system (*H*). This is described as the second law of thermodynamics for an open system and is shown below in Equation (4-26).

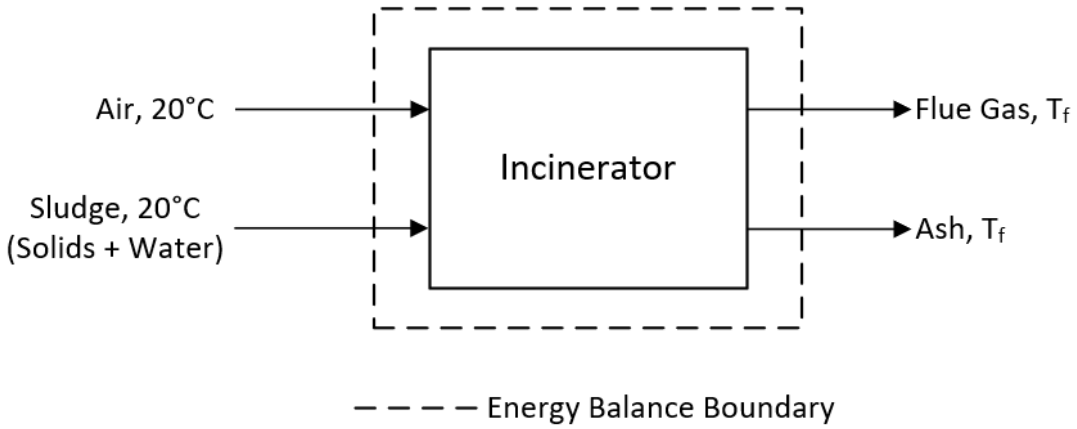

Figure 4-4: Energy balance on the incinerator.

$$\frac{dE}{dt} = \sum_{in} \dot{m}_i \left(h_i + \frac{{v_i}^2}{2} + g z_i\right) - \sum_{out} \dot{m}_j \left(h_j + \frac{{v_j}^2}{2} + g z_j\right) + Q + W \qquad \textbf{(4-26)}$$

Under the steady-state assumption, no energy accumulates in the system and $^{dE}/_{dt}$ equals zero. The incinerator does no work and is presumed to be a well insulated system, making Q and W both zero as well. The change in enthalpy is much larger than the change in kinetic and potential energy meaning that the kinetic and potential energy can be neglected entirely. All of these factors can be used to simplify Equation (4-26) to Equation (4-27) which states that the change in enthalpy (ΔH) is equal to zero.

$$0 = \sum_{out} \dot{m}_j h_j - \sum_{in} \dot{m}_i h_i = \Delta H \qquad \textbf{(4-27)}$$

For an enthalpy balance, the path taken to get from the initial enthalpy state to the final enthalpy state does not matter as long as it begins at the initial state and ends at the final state. For this reason, the path taken will be split into combustion (ΔH_1), evaporation (ΔH_2), and product heating (ΔH_3) and can be seen below in Figure 4-5. Equation (4-27) can now be expanded to Equation (4-28), which incorporates the path taken from the initial to the final state.

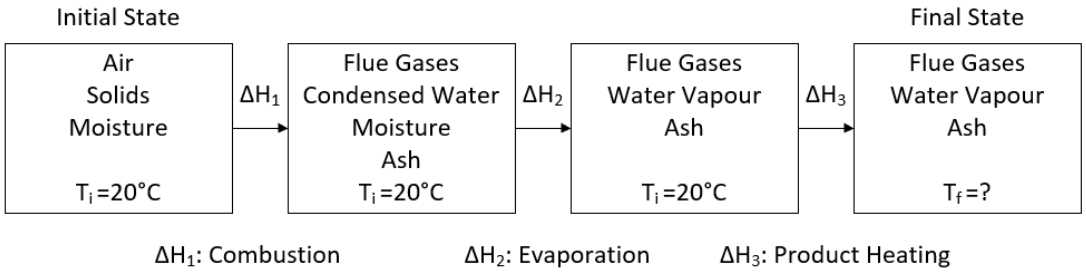

Figure 4-5: Path taken for adiabatic flame temperature model.

$$0 = \Delta H = \Delta H_1 + \Delta H_2 + \Delta H_3 \quad \textbf{(4-28)}$$

As shown below in Equation (4-29), the energy from combustion is a negative value because combustion is exothermic and is simply the product of the mass of dried solids entering the incinerator ($\dot{m}_{sol}$) and the higher heating value (*HHV*) which is obtained from the bomb calorimeter.

$$\Delta H_1 = -\dot{m}_{sol} HHV \quad \textbf{(4-29)}$$

The combustion vessel used in the bomb calorimeter is a closed system and as a result, the water vapour that is formed during the combustion of dry solids condenses. In an open system such as in an incinerator, the water vapour remains a gas and exits the system with the rest of the flue gas. Therefore, as shown in Equation (4-31), the energy required to evaporate the condensed water ($\dot{m}_H$) as well as the energy required to evaporate the moisture ($\dot{m}_{H2O}$) in the sludge cake must be accounted for by using the latent heat of vaporization of water (Δh_{Evap}) at 20°C.

$$\Delta H_2 = (\dot{m}_H + \dot{m}_{H2O})\Delta h_{Evap} \quad \textbf{(4-31)}$$

The products from combustion are composed of the flue gases and the ash. The product heating is shown below in Equation (4-32) and consists of the mass of the products

output from the system ($\dot{m}_{prod}$), the initial (T_0) and final temperature (T_f), and the average specific heat ($\bar{C}_p$) over those temperatures.

$$\Delta H_3 = \sum_{prod} \dot{m}_{prod} \bar{C}_p (T_f - T_0) \quad \textbf{(4-32)}$$

Combining Equations (4-28), (4-29), (4-30), and (4-31), results in Equation (4-33), which can be rearranged to solve for the final temperature as shown in Equation (4-34).

$$0 = -\dot{m}_{sol} HHV + (\dot{m}_H + \dot{m}_{H2O}) \Delta h_{Evap} + \sum_{prod} \dot{m}_{prod} \bar{C}_p (T_f - T_0) \quad \textbf{(4-33)}$$

$$T_f = T_0 + \frac{\dot{m}_{sol} HHV - (\dot{m}_H + \dot{m}_{H2O}) \Delta h_{Evap}}{\sum_{prod} \dot{m}_{prod} \bar{C}_p} \quad \textbf{(4-34)}$$

4.2.1 Combustion Mass Balance

The components of the solid portion of sludge are carbon (C), hydrogen (H), nitrogen (N), sulfur (S), oxygen (O), and fixed solids. During combustion, the CHNS are oxidized to form carbon dioxide (CO_2), water (H_2O), nitric oxide (NO), and sulfur dioxide (SO_2), respectively. These reactions are found below in Equations (4-35), (4-36), (4-37), and (4-38). The mass balance is performed on a basis of one gram of dry solid per second, and the amount of C (*c*), H (*h*), N (*n*), and S (*s*) are obtained by converting the results of the CHNS analysis into moles.

$$cC + O_2 \rightarrow cCO_2 \quad \textbf{(4-35)}$$

$$hH + \frac{1}{2} O_2 \rightarrow \frac{h}{2} H_2O \quad \textbf{(4-36)}$$

$$nN + \frac{1}{2} O_2 \rightarrow nNO \quad \textbf{(4-37)}$$

$$sS + O_2 \rightarrow sSO_2 \quad \textbf{(4-38)}$$

The mass of fixed solids is determined by the furnace test, and the O content is determined by difference. Similar to the other components, the amount of O (*x*) is

determined by converting its mass to moles. The O in the sludge is used during combustion and any remaining O required is provided from air, which contains 3.76 moles of diatomic nitrogen (N_2) for every mole of diatomic oxygen (O_2). The amount of O_2 required (*b*) can be determined by performing a mass balance shown Equation (4-39). The overall combustion reaction is shown below in Equation (4-40).

$$b = c + \frac{h}{2} + \frac{n}{2} + s - \frac{x}{2} \quad \textbf{(4-39)}$$

$$cC + hH + nN + sS + xO + Fixed\ Solids + bO_2 + 3.76bN_2$$

$$\rightarrow cCO_2 + {}^{h}/_{2}\, H_2O + nNO + sSO_2 + Ash + 3.76bN_2 \quad \textbf{(4-40)}$$

To account for 20% excess air and moisture in the sludge, the O_2 and N_2 in the reactants must be multiplied by 1.2 and liquid water must be added to the reactants in Equation (4-40), resulting in Equation (4-41). The amount of liquid water in the sludge (*w*) is determined by the wt.% solids of the sludge. Equation (4-41) can be used to obtain the flowrates of all of the combustion products.

$$wH_2O_{(l)} + cC + hH + nN + sS + xO + Fixed\ Solids + 1.2(bO_2 + 3.76bN_2)$$

$$\rightarrow cCO_2 + w\,{}^{h}/_{2}\, H_2O + nNO + sSO_2 + Ash + 0.2bO_2 + 4.51bN_2 \quad \textbf{(4-41)}$$

Chapter 5: Results and Discussion

5.1 Physical Characteristics of Aquaculture Sludge

Aquaculture sludge is not a homogeneous solid as shown in Figure 5-1. Young broodstock sludge that has not been spun contains granular particles scattered amongst the viscid material of the sludge. The granular material appears to consist of crystals of various shapes, sizes, translucency, and colour. Meanwhile, the viscid material is stringy, amorphous, and soft.

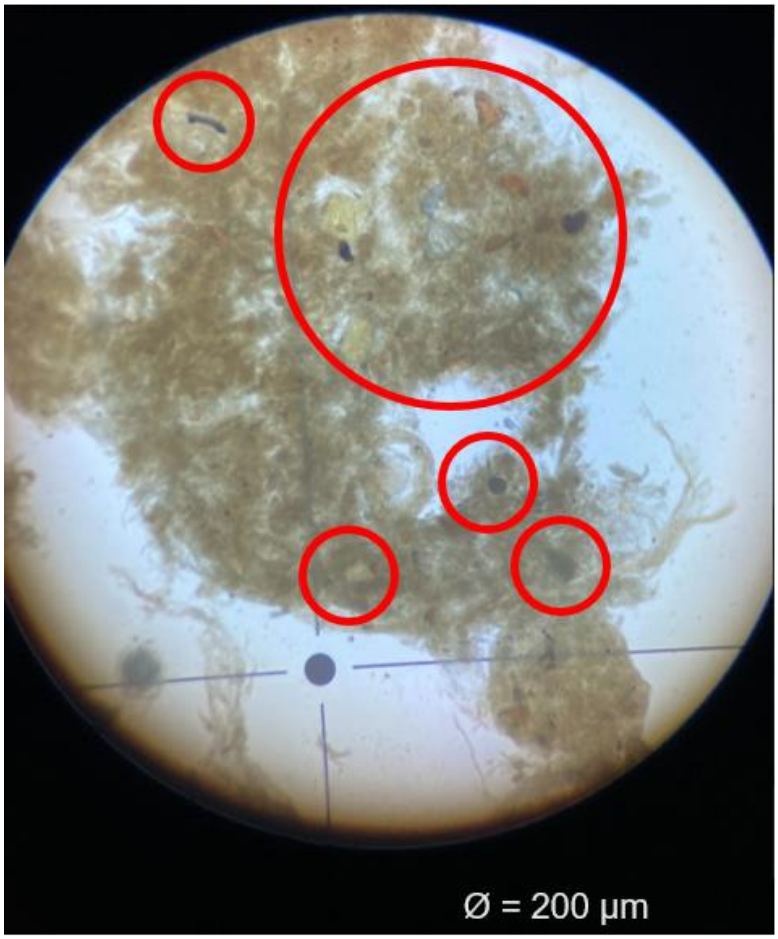

Figure 5-1: Microscopic photo of sludge that contains granular particles in the viscid material.

5.1.1 Particle Densities

By using the sucrose solution method, the viscid material was determined to have a density of approximately 1030 kg/m^3 and the granular material to have an average density of 1150 kg/m^3. In 2003, researchers Patterson and Watts had also noticed that there were two types of micro-particles in aquaculture sludge (Patterson & Watts, 2003). They determined that the granular particles had an average density of 1150 kg/m^3, which is in accordance with our findings, however, they found that the viscid material was slightly denser at 1050 kg/m^3. As determined by using the liquid displacement method, the density of viscid material and granular particles when dried increased to 1216 kg/m^3, and 1570 kg/m^3, respectively. This increase is believed to come from the shrinkage of the solids when water trapped deep within them evaporates. Some of this water is a part of the cells and their surrounding extracellular polymeric substances.

5.1.2 Granular Particle Size Analysis

A particle size analysis was not performed on the viscid material because its particles are small, stringy, and tangled together. For the software to work there must be a clear boundary between the particles, and the viscid material has too much overlapping. Additionally, the particle diameter is calculated under the assumption that projected area is circular, which is not a good assumption for the long and stringy particles that make up the viscid material. A particle distribution analysis was able to be performed on the granular particles because they are easy to separate from one another and have a projected area that closely resembles a circle. Figure 5-2 shows both types of solid under a microscope.

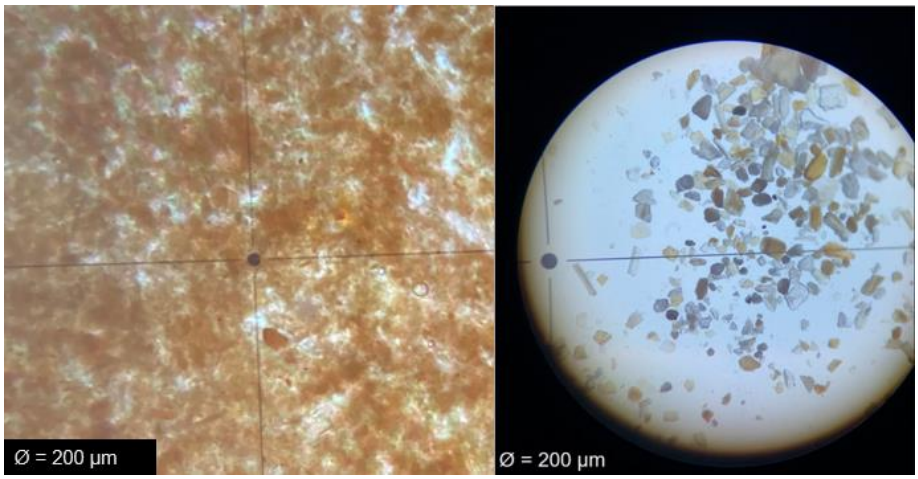

Figure 5-2: Microscopic images of viscid material (L) and granular particles (R).

After analysing 253 granular particles using multiple samples and photographs, it was determined that the diameter range that contained the most particles was 0 to 50 µm. Although the 0 to 50 µm diameter group contained the most particles by almost twice as much as the next highest group, it also contains the lowest volume of particles. This can be seen in Figure 5-3 and Figure 5-4, respectively. Assuming sphericity, the volume is a function of the radius cubed, and as a result, the smaller diameter particles make up much less of the granular material's volume. The volume based median value, known as the D_{50}, was determined to be 400 µm. The D_{50} is the diameter where 50% of the volume is made up of particles smaller than this diameter.

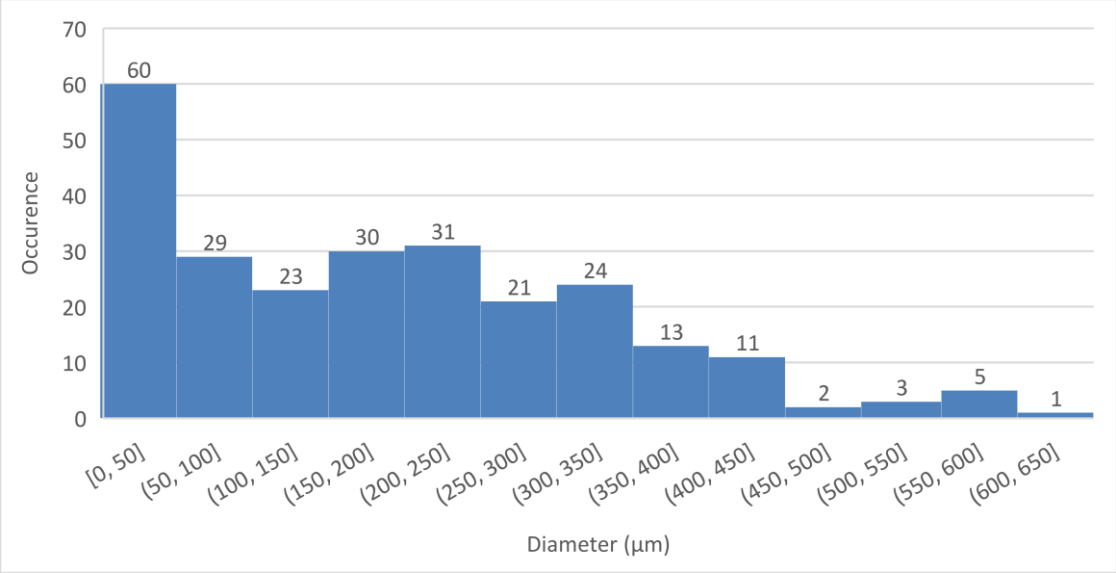

Figure 5-3: Number-frequency histogram for the size distribution of granular particles.

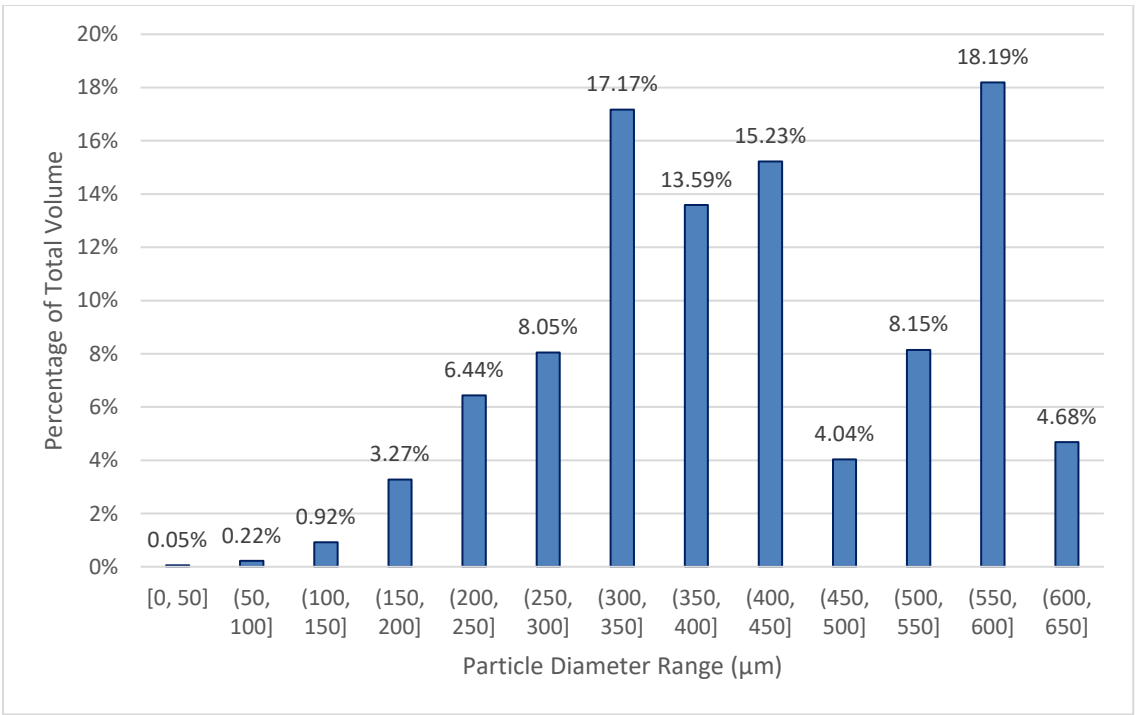

Figure 5-4: Volume-frequency histogram for the size distribution of granular particles.

5.2 Chemical Characteristics of Aquaculture Sludge

Although young and adult broodstock sludge have a different physical appearance, the results from the CHNS analysis and furnace test, shown in Table 5-1, indicate that they have the same organic composition. Young broodstock sludge was determined to be approximately 75% organic and 25% fixed solids and similarly, adult broodstock sludge was approximately 72% organic and 28% fixed solids. When a furnace is used to burn off the organic content in sludge, the term "fixed solids" is used in place of inorganic solids because some mineral salts can decompose under high temperatures. This causes the fixed solids content to vary slightly compared to the true inorganic solids content. Accordingly, when dried, both sludge types have the same HHV of approximately 16 kJ/g.

Table 5-1: Composition of sludge.

Sludge Type	Composition (wt.%)					
	C	H	N	S	O	Fixed Solids
Young Broodstock	37.1 ± 0.2	4.8 ± 0.1	5.2 ± 0.1	1.9 ± 0.4	25.6 ± 0.5	25.4 ± 0.3
Adult Broodstock	39 ± 2	5.0 ± 0.2	5.1 ± 0.3	1.9 ± 0.3	21 ± 2	28.1 ± 0.3

Although both sludge types have approximately the same percentage of fixed solids, there was a difference in their trace metal concentration. The trace metal analysis tested a variety of metals, however most had a negligible concentration and as a result, only the metals with a significant concentration are included in Table 5-2. Furthermore, only one sample per sludge type was tested, and entirety of the trace metal analysis results can be

found in Appendix A. Shown in Table 5-2, the results from this test indicate that the trace metals in the sludge are primarily dietary metals that are found in the feed. With the exception of calcium, strontium, and zinc, the dietary metal concentration was significantly higher in the adult broodstock sludge compared to the young broodstock sludge. The sodium concentration was found to be remarkably higher in the sludge from the adult broodstock and this can be explained by the system water that saturates the sludge. The system that houses adult broodstock contains brackish water and has a salinity of around 6 ppm, which is much higher than the young broodstock's system water.

Table 5-2: Trace metals in sludge.

Analytes	Units	Adult Broodstock Sludge	Young Broodstock Sludge
Aluminum	mg/kg	608	270
Calcium	mg/kg	79,900	109,000
Iron	mg/kg	4,630	1,310
Magnesium	mg/kg	4,720	3,160
Manganese	mg/kg	448	189
Potassium	mg/kg	1390	310
Sodium	mg/kg	12,300	2,780
Strontium	mg/kg	214	317
Zinc	mg/kg	986	837

5.2.1 Identification of the Particles

Various tests were done to determine the nature of the particles. As expected, the viscid material appears to be primarily organic matter. The CHNS and fixed solids results seen

in Table 5-3 show that the viscid material is around 86% organic and of that 52% is carbon. As shown in Table 5-4, the viscid material's HHV was determined to be 24.0 ± 0.3 kJ/g and is attributed to its high organic content. The fixed solids present in the viscid material is likely a result of small granular particles in the viscid material or dissolved solids that precipitated when the viscid material was dried prior to its analysis. The viscid material was approximately 10 wt.% solids before it was dried meaning that 90% of its weight was from trapped water which contained dissolved solids. Magnesium chloride, calcium chloride, sodium bicarbonate, and sodium hydroxide are added to the RAS water to control water quality and will precipitate back to their solid form as the water in the viscid material evaporates. Results from the trace metal analysis shown in Table 5-5 show that the inorganic portion of the viscid material is mostly calcium, magnesium, and sodium compounds, which is in accord with the water treatment compounds added.

Table 5-3: Viscid material and granular particle composition from young broodstock sludge.

	Composition (wt.%)					
Particle	**C**	**H**	**N**	**S**	**O**	**Fixed Solids**
Viscid	52.1 ± 0.4	6.27 ± 0.05	4.3 ± 0.1	1.95 ± 0.03	21.3 ± 0.6	14.1 ± 0.4
Granular	22.6 ± 1.3	2.6 ± 0.3	4.8 ± 0.2	0.7 ± 0.2	11.8 ± 1.9	57.5 ± 1.1

Table 5-4: HHV of aquaculture sludge and its two parts.

Sludge Type	HHV (kJ/g)
Adult Broodstock	16.4 ± 0.3
Young Broodstock	16.3 ± 0.1
Granular Particles	8.6 ± 0.8
Viscid Material	24.0 ± 0.3

Table 5-5: Notable compounds from the trace metals analysis. The complete list of metals tested can be found in Appendix A.

Analytes	Units	Granular	Viscid
Aluminum	mg/kg	148	130
Calcium	mg/kg	183,000	66,700
Iron	mg/kg	810	740
Magnesium	mg/kg	4,430	3,380
Manganese	mg/kg	242	148
Potassium	mg/kg	340	560
Sodium	mg/kg	4,630	9,940
Strontium	mg/kg	240	120
Zinc	mg/kg	722	664

For the granular particles, the CHNS and furnace tests have determined that the granular particles mostly consist of fixed solids, however, there does appear to be some organic matter. The HHV was determined to be 8.6 ± 0.8 kJ/g of dry solids, which would suggest that the granular particles are mostly inorganic with a small fraction being organic. The percentage of granular solids in aquaculture sludge can be calculated by using the HHV or elemental composition values for sludge, viscid material, and granular particles. The calculated mass percentage of granular particle in sludge based off the carbon, hydrogen, fixed solids, and HHV can be found below in Table 5-6. A description of the calculation for the mass fraction of granular particles in dry sludge can be found in Appendix C.

Table 5-6: Mass percentage of sludge that is granular particles based off elemental composition and HHV.

Based Off	wt.% of Granular Particles in Dry Sludge
Carbon	44 ± 7
Hydrogen	35 ± 7
Fixed Solids	31 ± 1
HHV	50 ± 1

It is suspected that the granular particles are remnants of feed that were eaten by the fish, but not completely digested. Based off the ingredients provided by the manufacturer, Skretting, the granular particles are likely made up of bonemeal, calcium carbonate ($CaCO_3$), and grain. To determine what percentage of the granular particles are bone, $CaCO_3$, or any other mineral with ionic bonds, the granular particles were added to 1.21 mol/L of hydrochloric acid (HCl). Fifty-five percent of the granular particles dissolved and when dissolved, some particles were observed to release gas bubbles. This gas was likely carbon dioxide (CO_2) which is formed when $CaCO_3$ dissolves. CO_2 is also produced by calcination, which is when $CaCO_3$ decomposes at high temperatures. The release of CO_2 from calcination causes inorganic weight loss which increases the difference between fixed solids and inorganic solids content. Additionally, the trace metal results indicate that the granular particles contain a significant amount of calcium, which is found in $CaCO_3$ and bonemeal.

When the granular particles were stained with thionine, some brown flakes turned blue, which suggests that they are a neutral polysaccharide such as dextrin or starch grain (Patterson & Watts, 2003). Furthermore, the blue stained particles were not able to be

dissolved by the HCl, which is not an oxidizing agent and does not digest organic matter. For these reasons, it is believed that the granular particles are made up of bone, calcium carbonate, and grain. Patterson and Watts concluded that the granular particles consist of bone fragment, and indigestible heavy cellulose from wheat. In their scientific article there was no mention of $CaCO_3$, however the fish from their trial were given feed from a different supplier and fish feed formula could have changed in the past 19 years since their findings.

5.3 Jar Test

A jar test was performed to determine which dose of chemical conditioners caused the sludge to form large flocs and decrease the free water's turbidity, which is measured in formazine attenuation units (FAU). To account for sludges of different solids content, the chemical conditioners were dosed in milligram of chemical conditioner per gram of dry solid in the sludge.

5.3.1 Coagulant

Not very much coagulant is required for flocs to form, and for the turbidity of the free water to rapidly decrease. Shown in Figure 5-5, FS and PAC displayed a similar trend for turbidity and at around 150 mg/g solid the turbidity was at its lowest. Any doses greater than this created smaller flocs and there appeared to be more microparticles in suspension. The only noted difference is that FS stains the water red when overdosed and is denser than PAC. The density of FS was 1.50 g/mL meaning that less is required to reach the ideal dose compared to PAC which has a density of 1.37 g/mL.

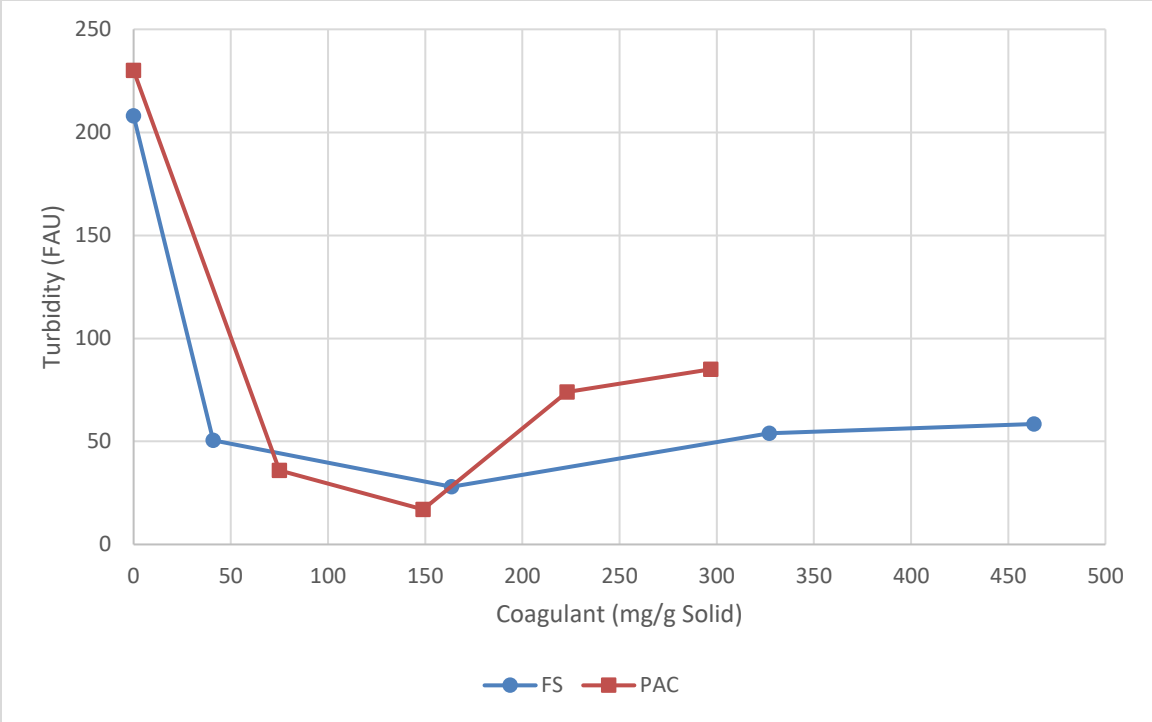

Figure 5-5: Turbidity of the free water when coagulants were added to sludge.

5.3.1.1 Solids Content Effect on Coagulant Dosing

To determine if the solid content in the sludge impact the dosage of coagulants, the tests were repeated with sludges of varying concentrations of total suspended solids (TSS). Due to the varying TSS, the sludge samples had a large difference in initial turbidity, so the turbidity was measured in the percent reduction. The turbidity value itself is not overly important, the point where it reaches the lowest is. Shown in Figure 5-6, even with different initial TSS content, the turbidity of all the samples followed the same trend and reached its lowest point at around 150 mg coagulant/g solid, which means that coagulants are unaffected by the total amount of solids in the sample.

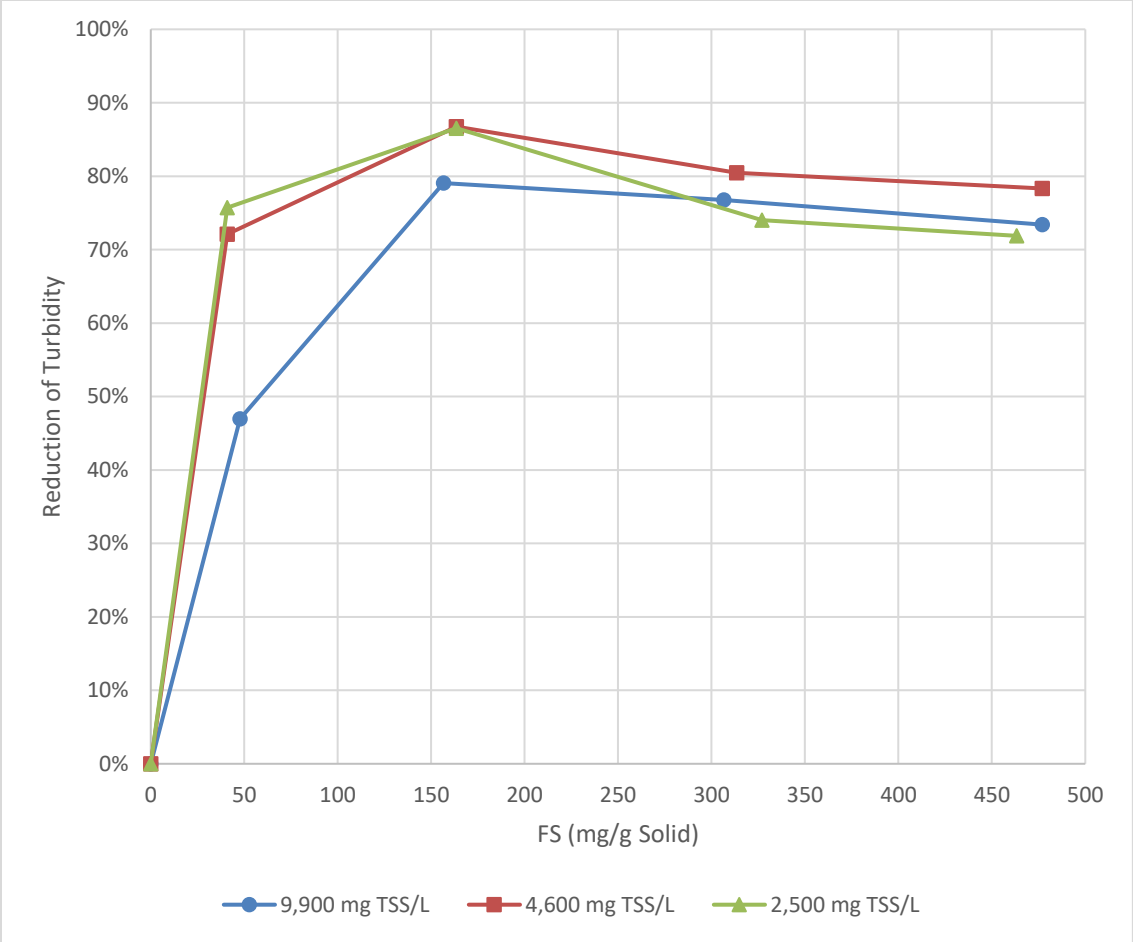

Figure 5-6: Turbidity of the free water when coagulant was added to sludge of varying TSS.

5.3.1.2 Particle Size Effect on Coagulant Dosing

To determine if the size of particles impacts the dosage of coagulants, the trials were repeated with sludge that had been shredded by a blender. In comparison to Figure 5-5, and Figure 5-6 located above, the lowest point on Figure 5-7 was shifted to the right. The turbidity reached its lowest point at around 250 mg coagulant/g solid instead which is a 66% increase from the non shredded optimal dose of 150 mg coagulant/g solid. This is logical, as coagulants function by neutralizing the negative charge of the solid particle by

coating its exterior and preventing the particles from repelling each other. When larger particles are broken down into smaller particles, the surface area to volume ratio increases and more coagulant is needed to neutralize the same volume of particles. This highlights the importance of preserving the sludge as it is transported from settling tank or filter to effluent treatment in order to prevent the particle size from degrading.

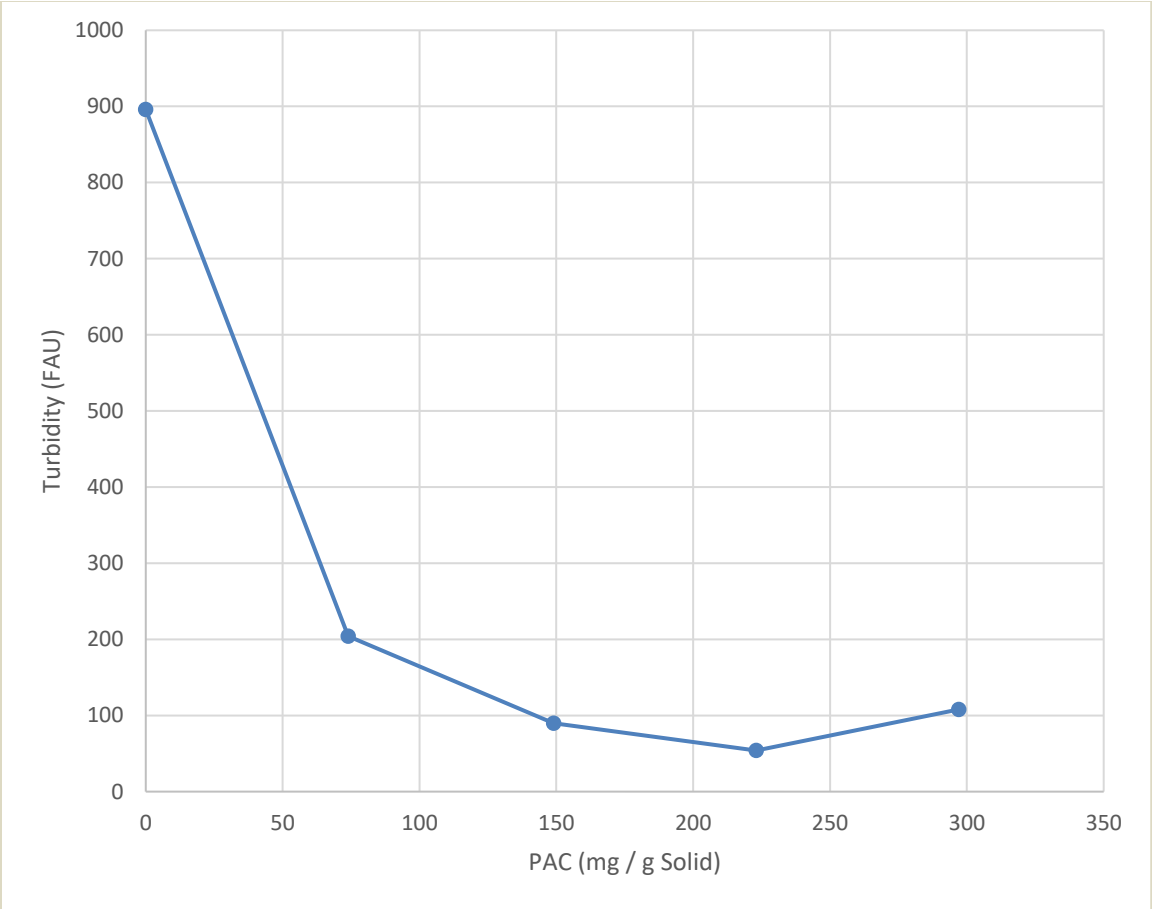

Figure 5-7: Turbidity of the free water when coagulant was added to shredded sludge.

5.3.2 Flocculant

PAM worked quickly after addition to create large flocs and yielded similar results when used with FS and PAC. Shown below in Figure 5-8 and Figure 5-9, the area that had the lowest turbidity was past 150 mg coagulant/g solids and 1 mg flocculant/g solid for both contour plots. As a result, 150 mg coagulant/g solid and 1 mg PAM/g solid can be said to be the ideal dose because it is the point that uses the least amount of chemical conditioner while still providing the maximum flocculation and turbidity reduction. As previously mentioned, 150 mg coagulant/g solid was also the optimal dose of coagulants when the sludge was not dosed by PAM. It can be deduced that when used together, coagulants work independently from PAM and the coagulant dosing is independent from PAM dosing.

Solely adding PAM did not have any visual effect on the sludge as no flocs were formed and the turbidity remained unchanged. This determined that PAM does not function without the prior use of a coagulant and is used to increase the effectiveness of coagulants. PAM started showing results at very low doses and can be easily overdosed, especially if the sludge has a low TSS. Luckily overdosing PAM does not hinder flocculation or decrease turbidity, it simply increases the viscosity of the solution and is a waste of flocculant.

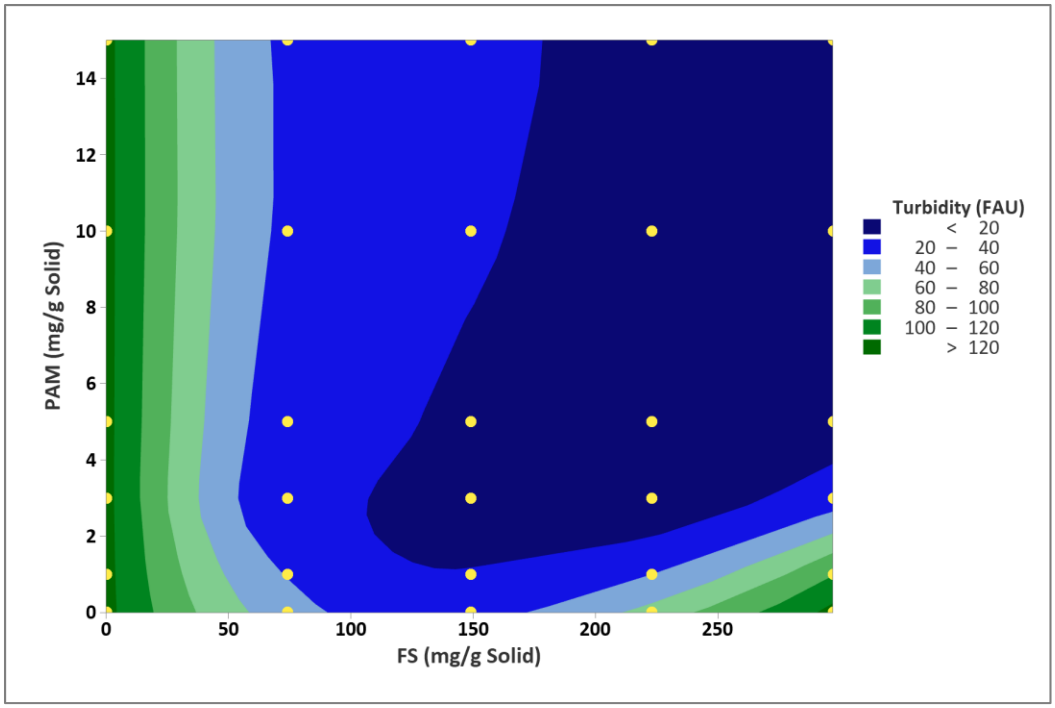

Figure 5-8: Turbidity of the free water when FS and PAM were added to sludge.

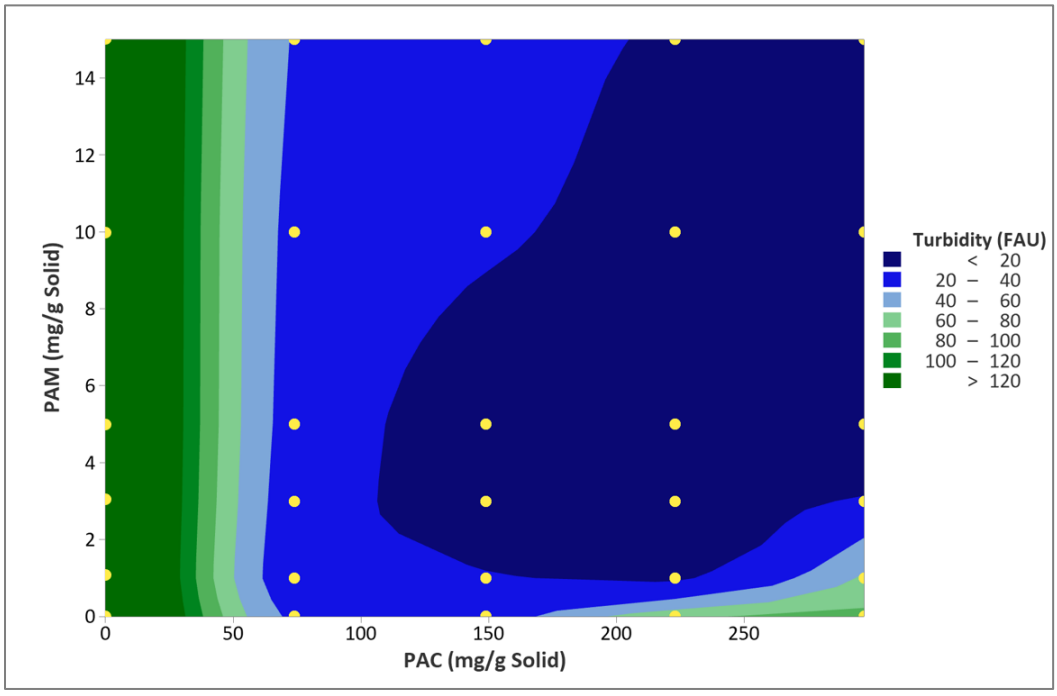

Figure 5-9: Turbidity of the free water when PAC and PAM were added to sludge.

5.3.2.1 Particle Size Effect on PAM Dosing

To determine the effect of particle size on PAM dosing, the previous test was repeated but using sludge that had been shredded in the blender. Shown below in Figure 5-10, the area that had the lowest turbidity was past 230 mg coagulant/g solid and 1 mg PAM/g solid. As a result, 230 mg coagulant/g solid and 1 mg PAM/g solid can be said to be the ideal dose because it is the point that uses the least amount of chemical conditioner while still providing the maximum flocculation and turbidity reduction. Even with a reduction in particle size, the optimal dose of PAM remained at 1 mg/g solid which further proves that the dosing of PAM is independent on the dosage of coagulant. This is logical, as the reduction of particle size that is done by the shredding is undone by the coagulant before the PAM is added.

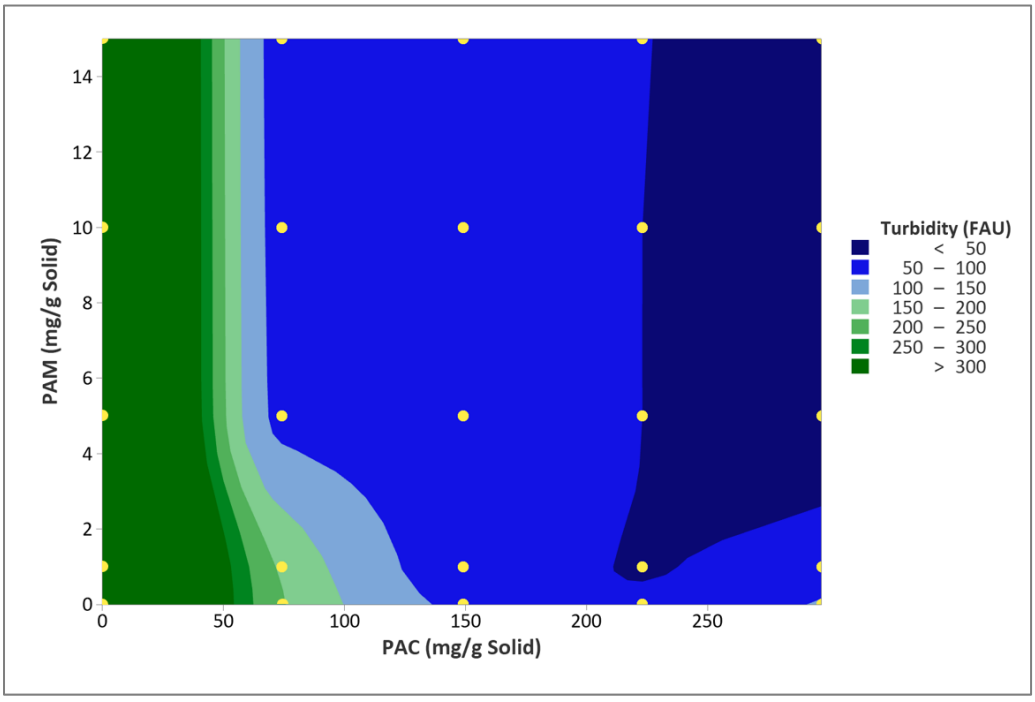

Figure 5-10: Turbidity of the free water when coagulant and PAM was added to shredded sludge.

5.4 Centrifugation of Aquaculture Sludge

5.4.1 Lab-Scale Centrifuge

Tests were run to determine the best operating conditions for the lab-scale centrifuge. Trials were performed to determine the impact that batch time and RCF have on the dewaterability. As shown below in Figure 5-11, when spun at increasing RCF, the wt.% solids increases up until 1,500-G where it reaches a plateau. Likewise, for batch times shown in Figure 5-12, the wt.% solids increased up until 15 min where it reaches a plateau. The subsequent trials were run for 20 min at 2,500-G because they are both well into their respective plateau regions.

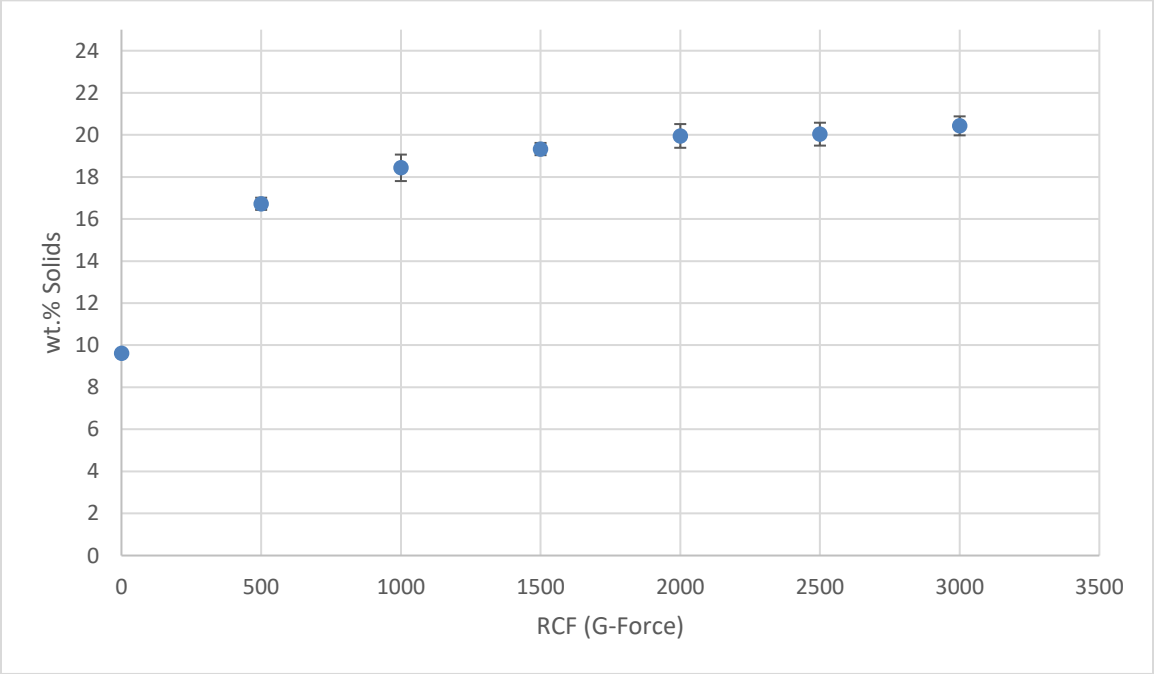

Figure 5-11: Effect of RCF on the solids content of the samples. Lab scale centrifuge, batch time of 20 minutes.

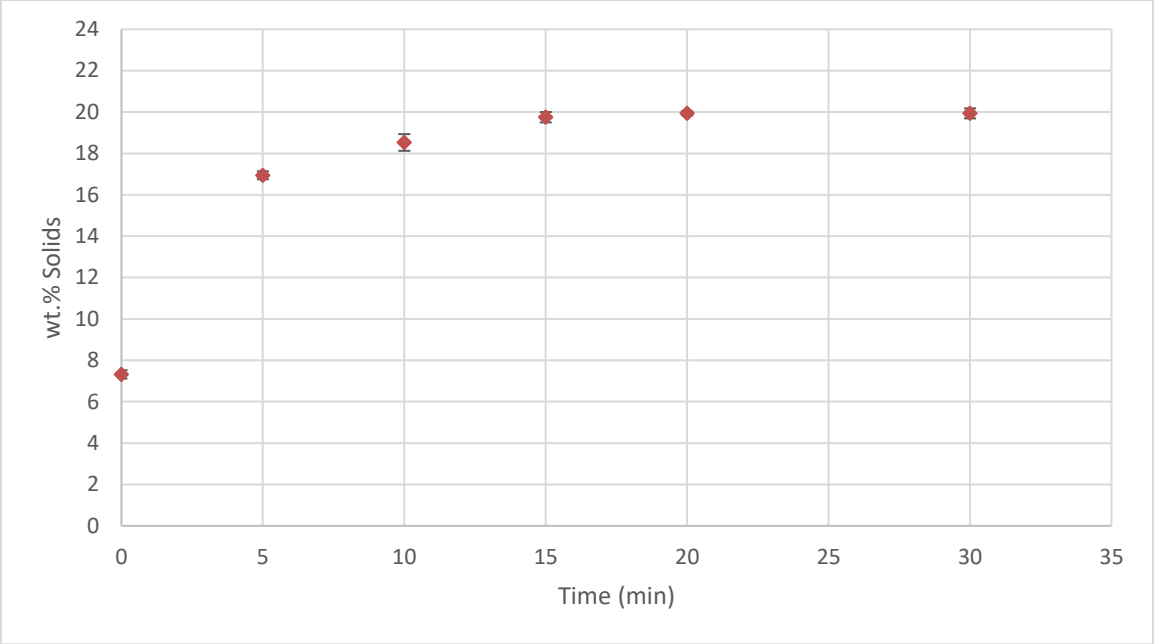

Figure 5-12: Effect of time on the solids content of the samples. Lab scale centrifuge, RCF of 2,500.

When fresh young broodstock sludge is used in the lab-scale centrifuge, the granular particles cannot escape the viscid material during centrifugation. Shown in Figure 5-13, this results in a cake that has very little difference between the bottom and the top, visually and in wt.% solids. This sludge dewaters to 19.3 ± 0.7 wt.% solids and has a slight moisture gradient of 23.2 ± 0.8 wt.% at the bottom of the cake and 14.8 ± 0.1 wt.% at the top.

Figure 5-13: Wet (top) and dried (bottom) young broodstock sludge after centrifugation.

During trials with adult broodstock sludge, it was discovered that adult broodstock sludge separates into two distinct layers during centrifugation. The denser granular particles form the bottom layer while the less dense viscid material make up the top layer. The adult broodstock sludge cake, which can be seen in Figure 5-14, was 18.8 ± 0.4 wt.% solids, however there was a moisture gradient throughout the cake. The granular layer was dryer at 38 ± 2 wt.% solids and the majority of the water in the cake was found within the viscid material layer, which was 9.1 ± 0.3 wt.%.

Figure 5-14: Wet (top) and dried (bottom) adult broodstock sludge after centrifguation.

Septic tank sludge also separated into two layers when spun, however the average moisture content varied depending on the depth that the sludge sample was taken from. Sludge sampled from the bottom of the septic tank (depth of 8 ft) dewatered to 33.9 ± 0.5 wt.% solids in the centrifuge while sludge from the top dewatered to 19.5 ± 0.8 wt.% solids. Shown in Figure 5-15, sludge from the bottom of the septic tank consisted of mostly granular particles and this was the reason it had such a high wt.% solids after centrifugation. Similar to in the centrifuged sludge cake, it would appear that the denser granular particles settle and make up the majority of the bottom layer of the septic tank.

Figure 5-15: Wet (L) and dried (R) sludge from the bottom of the septic tank after centrifugation.

Observations suggest that aquaculture sludge must be loose, shredded, or partially digested for the two particle groups to be able to freely separate. When the sludge is fresh, the granular material is encapsulated inside the fecal pellets and cannot freely move through the cake during centrifugation. Letting the sludge age in a tank allows for the granular particles to settle to the bottom and form a granular particle rich layer. This layer has high dewaterability, however allowing the sludge to digest causes the nutrients in the sludge to leech into the free water and would heavily pollute the environment if discharged.

Based off of findings from the literature review, the wt.% solids of the sludge was anticipated on being greater than the 19 wt.% solids. One possible explanation is intracellular water. In addition to bacteria cells, the sludge also contains plant cells which are found in the uneaten and undigested feed in the sludge. By mass, plant cells are 70%

water and are surrounded by a hard cell wall that cannot be broken by the centrifugal force (Cooper, 2000). This trapped intracellular water likely contributes to the centrifuged sludge cake's low wt.% solids and the solids content of the sludge cake is expected to increase if the cell walls are broken. Breaking the cell wall is a process known as lysis and can be achieved through heating, sonication, or the addition of chemicals (Islam, Aryasomayajula, & Selvaganapathy, 2017).

The granular particles alone could only be dewatered to 38 wt.% solids by centrifugation and this can be explained by the granular solids acting as a packed bed and absorbing water. The space in between the particles in a packed bed is known as void space and in this scenario the void space would be filled with water. A densely packed bed of irregular shaped sand particles with an average particle diameter of 400 μm has a voidage of 0.45 (Deng, et al., 2021). Assuming that the granular particles have a similar void space as sand, this would result in a packed bed that is 45% wt.% water. The remaining 18 wt.% of the water in the granular solids layer is possibly found inside the particles, as they are likely porous and absorb water.

5.4.1.1 Supernatant Phosphorous Concentration

In sludge, phosphorous is released by the solids in the form of orthophosphate. As a result, the water removed from deep within the solids during centrifugation is rich in orthophosphates and it was determined that the concentration in the supernatant was 130 ± 22 ppm. Coagulants often doubles as orthophosphate precipitation agents, so the test was repeated using sludge that was dosed with 150 mg FS/g solid, however results showed that the orthophosphates concentration remained the same as in the previous test.

High concentrations of chemical oxygen demand and TSS in wastewater are known to reduce the efficiency of chemical orthophosphate precipitation (Szabó, et al., 2008). As the sludge digests, it produces humic substances that react with iron and aluminium irons which leaves less ions available to react with the orthophosphate (WRF, 2019). Due to the high solids content of the sludge, it is likely that the concentration of compounds inhibiting orthophosphate precipitation is too high. Therefore, coagulants cannot be used to coagulate sludge and precipitate orthophosphate simultaneously.

Orthophosphate is a nutrient, and at high concentrations can cause excess algae blooms, known as eutrophication, in freshwater. Eutrophication can harm aquatic ecosystems in many ways, however the most notable is the depletion of dissolved oxygen in the water which makes it difficult for organisms to survive. As a consequence, aquaculture facilities must monitor and control the concentration of orthophosphate in their wastewater. Dewatering the sludge by centrifuge does reduce the disposal cost, however a new expense is introduced in the form of supernatant phosphorus treatment. At Johnson Lake Hatchery, orthophosphates will be removed by chemical precipitation by introducing PAC to the water. The active precipitating agent in PAC is the aluminium ion as it reacts with the orthophosphate to form solid aluminium (iii) phosphate, which can then be settled or filtered out of the water. Shown in Equation (5-1), for each mole of PAC ($Al_5(OH)_6Cl_9$), five moles of orthophosphate (PO_4^{3-}) can be removed.

$$Al_5(OH)_6Cl_{9(aq)} + 5PO_{4(aq)}^{3-} \rightarrow 5AlPO_{4(s)} \quad \textbf{(5-1)}$$

The daily dewatering of 30 tonnes of sludge initially at 2 wt.% to 20 wt.% will result in 27 tonnes of supernatant. Assuming a perfect stoichiometric conversion, 3.95 kg of PAC will be required to treat the orthophosphate in the supernatant. PAC is currently

purchased by Cooke at a cost $1.28/kg and this would equate to an annual cost of approximately $1,850.

5.4.1.2 Effect of Chemical Conditioners on Dewatering

Untreated young broodstock sludge can be dewatered to 19.3 ± 0.7 wt.% by centrifugation. However, when treated with the optimal dose of 150 mg of coagulant/g of dry solids and 1 mg PAM/g of dry solids, the solids content increased to 20 ± 1 wt.% after centrifugation. Although the average solids content did slightly increase with the addition of chemical conditioners, the difference between the two values is not statistically significant. Because of variations in sample composition and particle size distribution, the chemicals did not always have an effect on dewaterability. Due to the variability of results, negligible increase in wt.% solids, and cost, it is recommended not to use coagulants and flocculants for the dewatering of aquaculture sludge with a centrifuge. Chemical conditioners promote floc formation which increases the sludge's average particle size which expedites sedimentation, however due the large centrifugal force exerted on the sludge, sedimentation is not an issue in a centrifuge.

It was determined that shredded sludge could only be dewatered to 10.9 ± 0.3 wt.% solids. The small particles create smaller interstices that do not allow water to easily drain out of the sludge cake. When dosed with 230 mg coagulant/mg solid and 1 mg PAM/g solid, the solids content of the centrifuged sludge cake was improved to 16.0 ± 0.2 wt.% solids, which is less than the 19.3 ± 0.7 wt.% solids achievable for non-shredded sludge. The negative effect from shredding the sludge cannot be reversed by chemical

conditioners and the sludge should be gently transported from its holding tank to the centrifuge to avoid any particle size reduction.

5.4.1.2 Effect of Physical Conditioners on Dewatering

Adding sawdust to young broodstock sludge resulted in an increased dewaterability as the sludge yielded a higher wt.% solids after centrifugation. Increasing the ratio of sawdust to sludge increased the wt.% solids after centrifugation up until 1:4 (parts sawdust : parts solid). Further increasing the ratio past this point resulted in no further increase in dewaterability. As shown in Figure 5-16, the ratio of 1:4 used the least amount of sawdust while yielding the best results, and for this reason, it was deemed to be the optimal ratio. Although sawdust was able to increase the sludge from 20.34 ± 0.04 wt.% solids to 23.8 ± 0.32 wt.% solids, it was still not effective. The goal is to reduce the weight of the sludge transported offsite for disposal, but the extra water removed is not enough to overcome the increase of weight from adding sawdust. Sawdust would only be effective if instead of being trucked offsite, the sludge was instead disposed of onsite by a method such as landfilling or incineration.

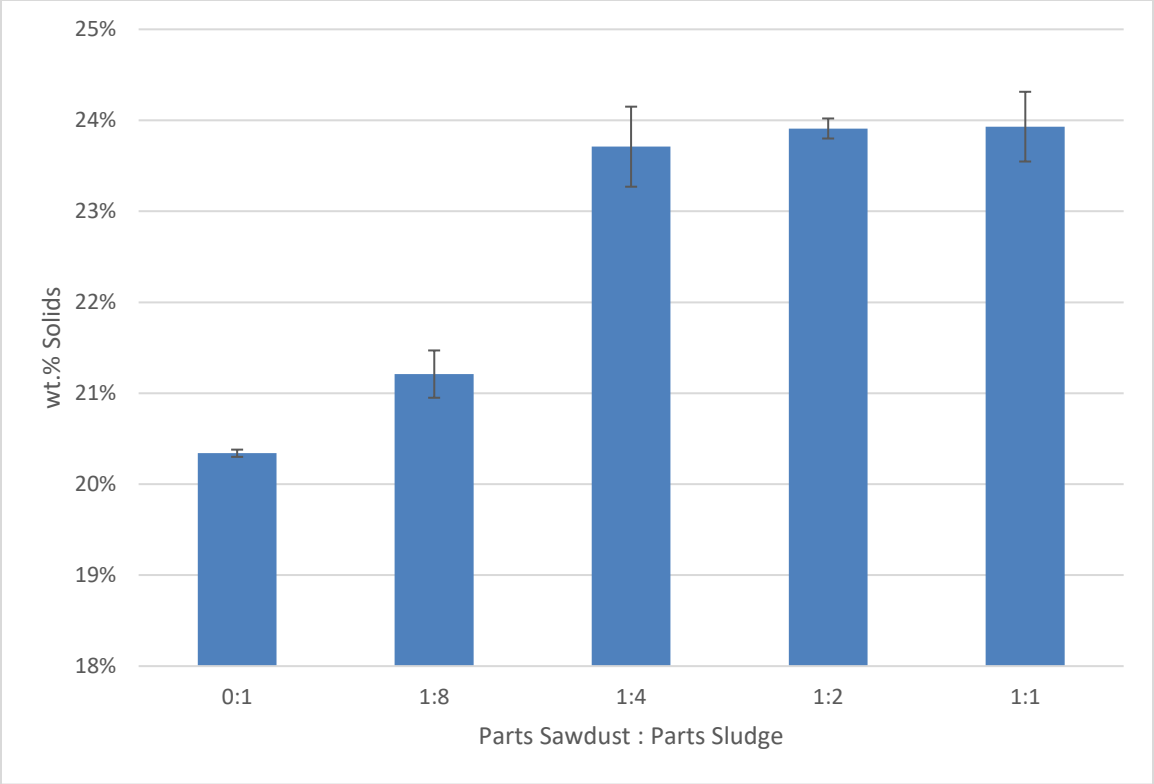

Figure 5-16: Sludge dewaterability using sawdust as a physical conditioner.

5.4.2 Pilot-Scale Centrifuge

When operated according to the manufacturer's guidelines, the centrifuge reaches the end of its batch cycle once 1 US gal of cake has accumulated in the 1.6 US gal bowl. The issue with operating in this manner is that there is no way to rid the remaining 0.6 US gal of free water from the bowl and consequently it mixes with the cake at 20 wt.% solids resulting in an approximate 15 wt.% solids cake. The centrifuge yielded a better dewaterability when the centrifuge ran until the inner radius of the cake (r) had reached the inner radius of the weir (r_i). A schematic for the centrifuge can be seen below in Figure 5-17.

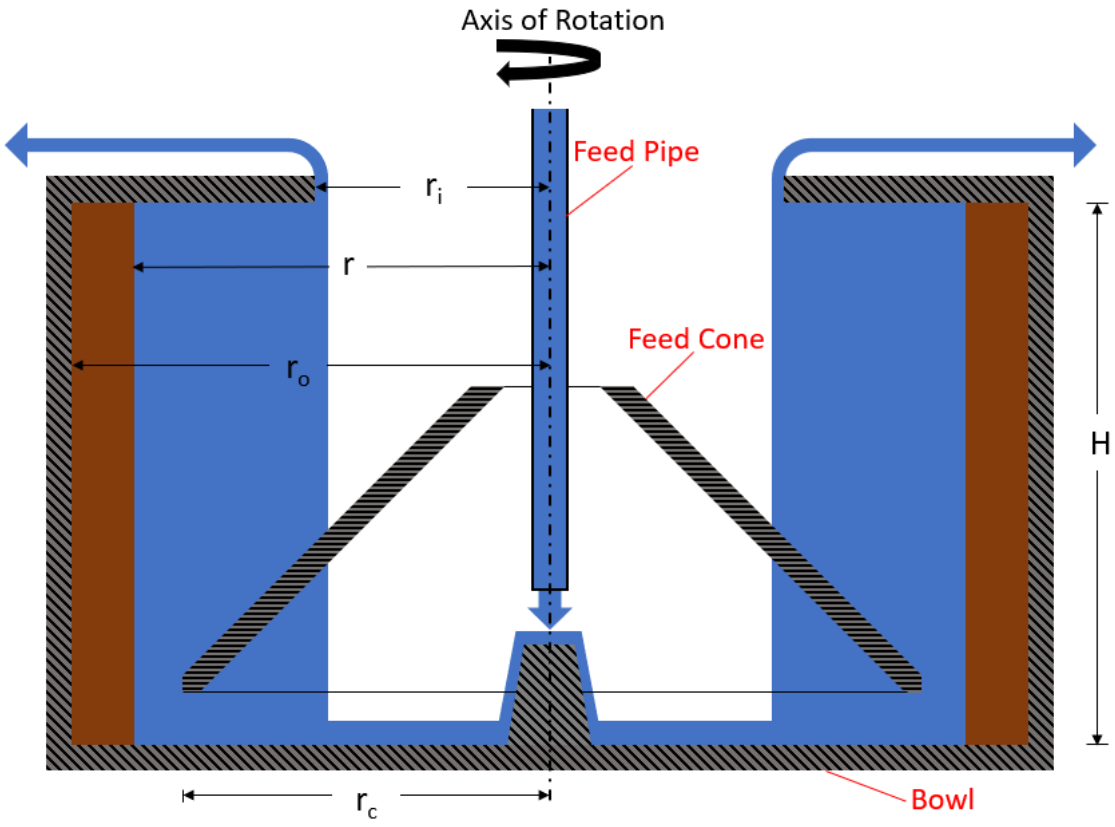

Figure 5-17: Schematic of a basket centrifuge.

A mass balance was performed around one of the trials on the basket centrifuge and a diagram for it can be found below in Figure 5-18. Twenty kilograms of young broodstock sludge initially at 9 ± 1 wt.% was fed into the centrifuge at a rate of 1 US gpm until the cake radius had reached the inner radius. The cake resulting from this trial was 23.1 ± 0.4 wt.% solids however it only contained 1.5 kg of the total 1.8 kg fed, yielding in a capture efficiency of 83%. In terms of water, only 5 kg of the total 18.2 kg fed remained in the bowl after operation which is a removal efficiency of 73%. Unlike the lab-scale centrifuge, the supernatant from this centrifuge was not free of solids and was 2.07 ± 0.01 wt.% solids. Fourteen percent, or 0.25 kg, of the total solids along with 67%, or 12.5 kg,

of the total water from the sludge ended up leaving with the supernatant. This means that the supernatant would have to be filtered or settled before it can be discharged with the rest of the effluent.

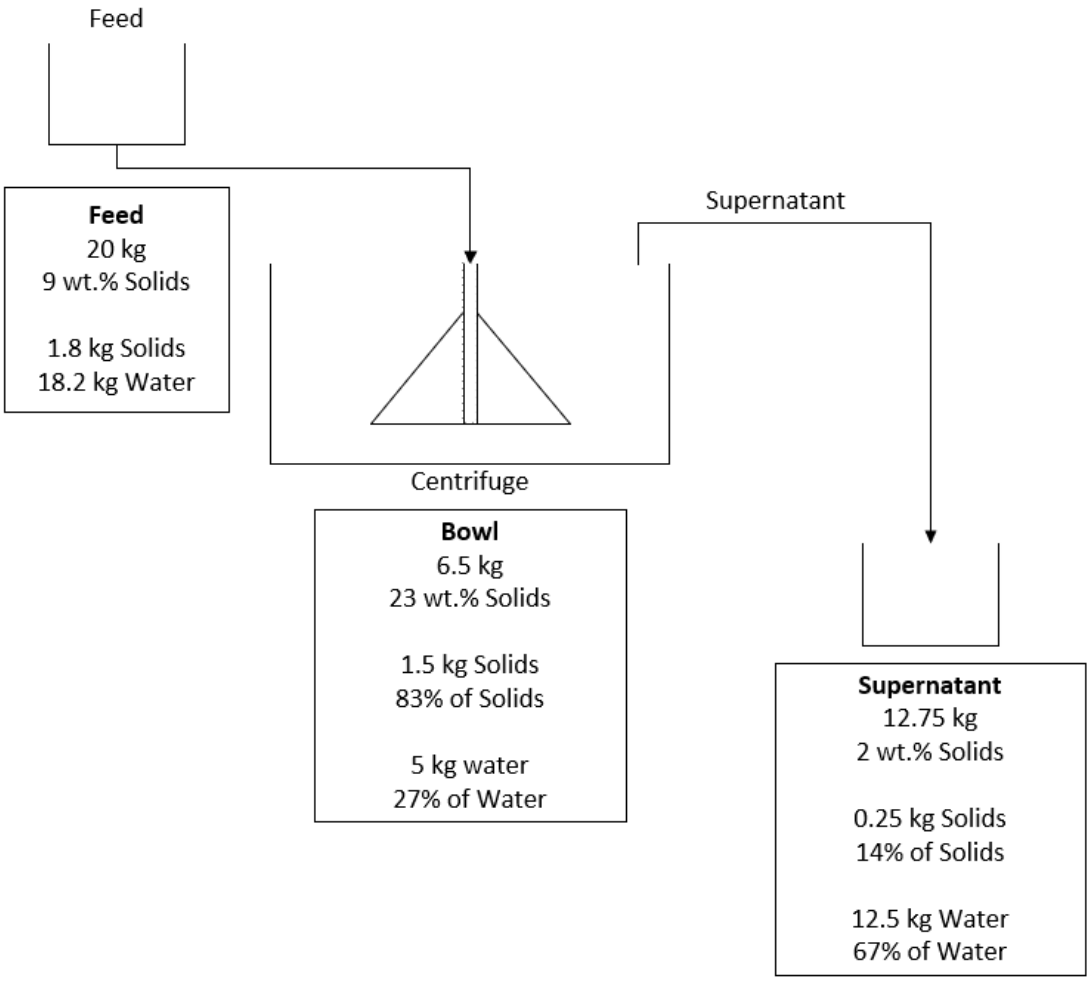

Figure 5-18: Pilot-scale centrifuge mass balance trial.

The pilot-scale centrifuge was able to dewater slightly better than the lab-scale centrifuge with one trial resulting in a cake with a 25.0 ± 0.8 wt.%. The main issue is that some solids leave with the supernatant, shown in Figure 5-19, and moreover this is what is causing the higher dewaterability. Unlike in the lab-scale unit, the young broodstock

sludge is able to separate into its two layers in the bowl of the pilot-scale unit. It is suspected that this occurs because the centrifugal force is instantaneous and because the particles have a much longer distance to travel. The granular material is much denser than the viscid material and settle first along the bottom of the bowl. As a result, the solids that leave with the supernatant is only viscid material, which has a much lower wt.% solids. This means that all of the higher wt.% solids granular material accumulates in the bowl, while a portion of the lower wt.% solids viscid material is not captured, and this causes the average wt.% solids of the cake to increase.

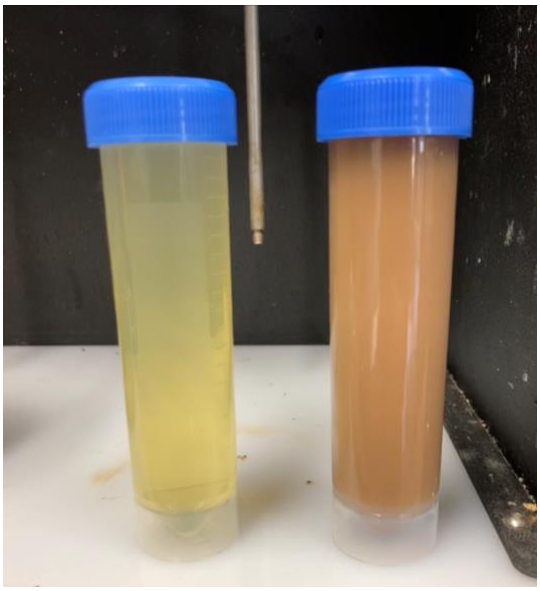

Figure 5-19: Lab-scale supernatant (L) compared to pilot-scale supernatant (R).

Decanter centrifuges are typically used to separate solids from liquids, while baskets centrifuges are mostly used to capture solid particles and produce a liquid stream that is free from solids. The cost of a basket centrifuge is a fraction of what a decanter centrifuge costs and if a basket centrifuge yields favourable dewatering results, they can be implemented at a hatcheries at a more affordable cost. Nevertheless, results suggest

that they are not suitable for sludge dewatering. Suggested methods to improve the operation of basket centrifuges can be found later in section 5.4.2.2.

5.4.2.1 Capture Efficiency Prediction

The predicted capture efficiency of the centrifuge was modeled in order to explain the results obtained from the trials. The model accounts for complete mixing that would occur under turbulent flow conditions and for no mixing which would occur under laminar flow conditions. The two conditions were used because in real world conditions there is some degree of mixing and therefore the actual curve for the capture efficiency is somewhere between the laminar and turbulent conditions that are shown in Figure 5-20 as the solid and dashed line, respectively. According to the model, the capture efficiency with no mixing and complete mixing are very similar and therefore either can be used to predict the capture efficiency.

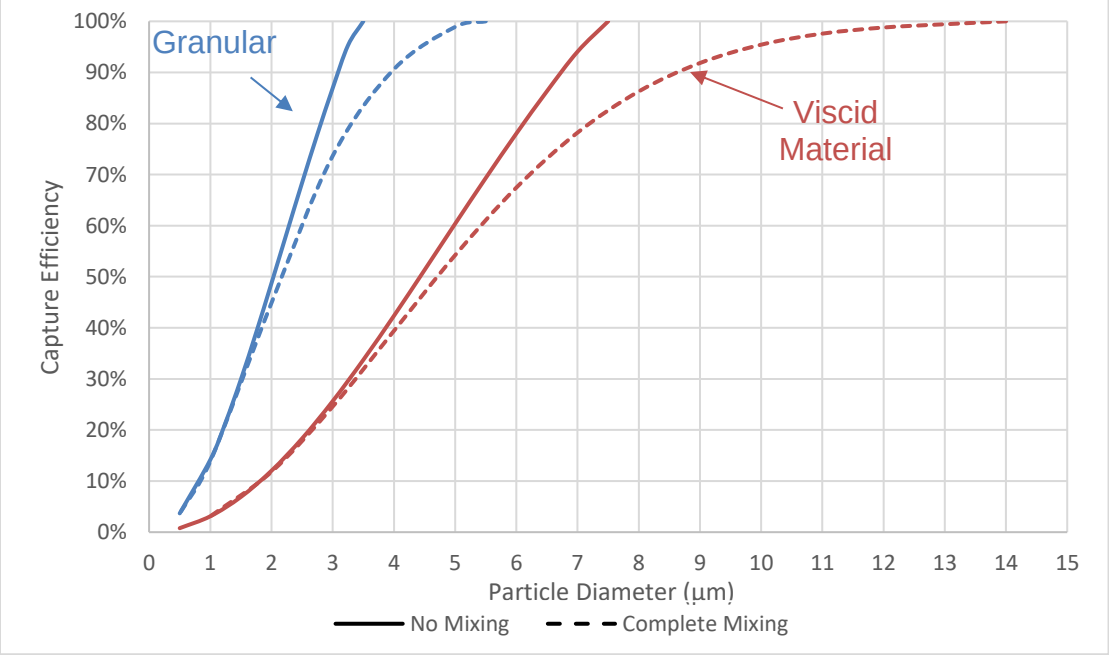

Figure 5-20: Capture efficiency of the basket centrifuge as predicted by the model.

The overall capture efficiency of the pilot-scale centrifuge during the mass balance trial was recorded to be 83%. The supernatant contained no granular particles, which means that their specific capture efficiency was 100%. Assuming the viscid material accounts for 65% of the mass of the solids would result in the viscid material having a capture efficiency of approximately 45%. Based off of predictions from the model, the viscid material would have to have a mean particle size of 2 μm to achieve this capture efficiency. Although a particle size analysis was not performed on the viscid material, when viscid material was observed under the microscope its particles appeared to be larger than 4 μm.

Some factor is believed to be reducing the centrifuge's capture efficiency. One factor that could impact the settling of the particle is their shape. The sludge particles vary in shape and the drag coefficient is greater for non-spherical particles. If the settling particle has a Re that is less than 0.1, the shape has no effect on the particles drag coefficient (Levenspiel, 2014). A particle's Re is proportional to its size, and as shown below in Figure 5-21, all the particles that have a capture efficiency less than 100% have a Re that is much less than 0.1, and therefore their low sphericity does not impact their settling. Once the particles reach a size where their drag coefficient is affected by their shape, they are already at a size where they easily settle and have a capture efficiency of 100%. For this reason, the shape of the particles is not what is causing the capture efficiency to be less than predicted.

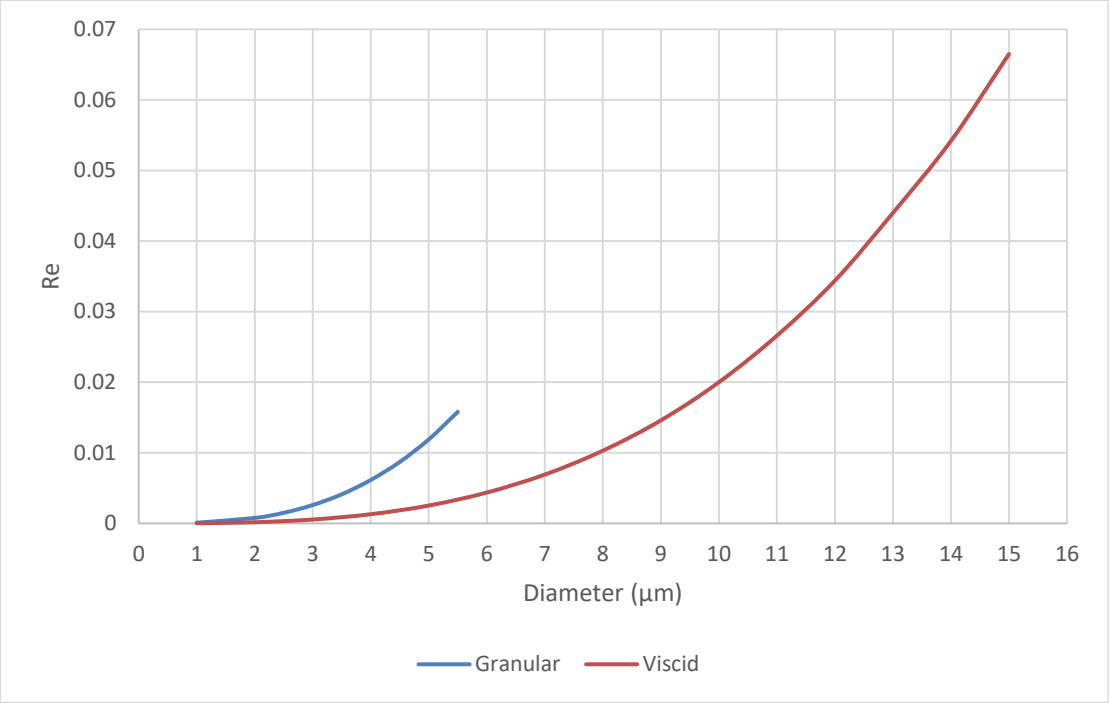

Figure 5-21: Reynolds number both types of particles at their terminal settling velocity.

As previously mentioned, if the centrifuge is operated until 1 US gal of cake has accumulated in the bowl, the remaining 0.6 US gal of free water mixes with the cake and this significantly lowers its wt.% solids. To avoid this, the centrifuge was run until the bowl was completely filled with solids, however this is what is believed to have caused the reduced capture efficiency. Eventually the inner cake radius (r) would reach the outer radius of the feed cone (r_c) and plug the bottom of the feed cone. This would cause the feed to exit the top of the feed cone which significantly reduces the time that the particles had to settle and causes solid entrainment in the supernatant.

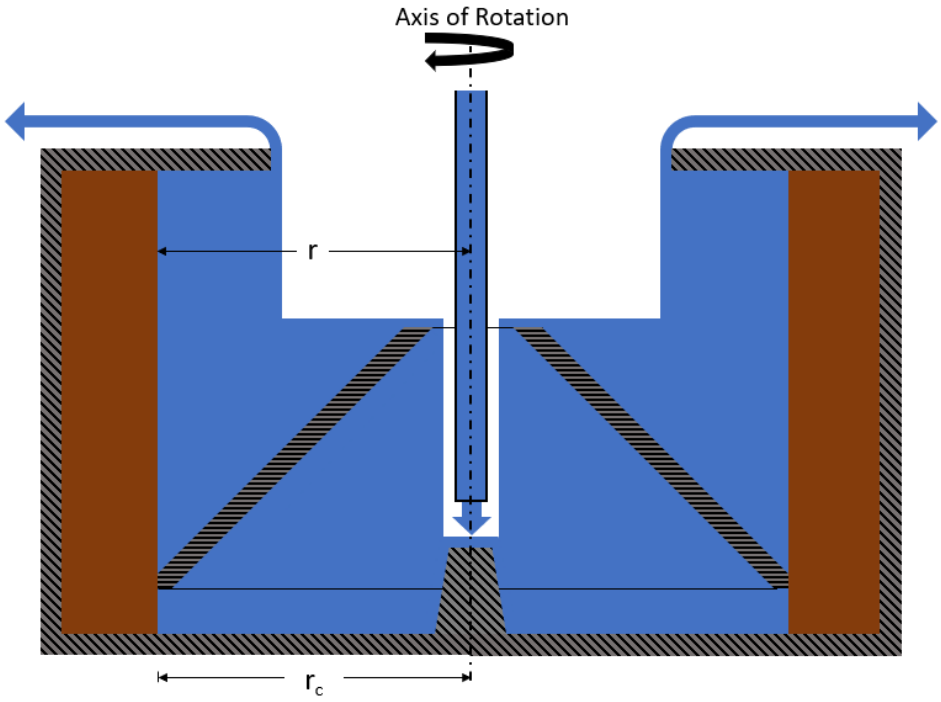

Figure 5-22: Sludge cake plugging the bottom of the feed cone and reroutes the feed to exit the top of the feed cone.

5.4.2.2 Suggested Modifications to Improve the Basket Centrifuge

To prevent the bottom of the feed cone from plugging, it is suggested that the outer radius of the cone is decreased to match the inner radius of the weir (r_i), as shown in Figure 5-23. With this change, the bowl will become full just as the bottom of the feeding cone is plugged. One potential downside to running the centrifuge until the bowl is full is that as the cake radius approaches the inner radius of the weir, the axial fluid velocity greatly increases and might cause particle entrainment in the supernatant.

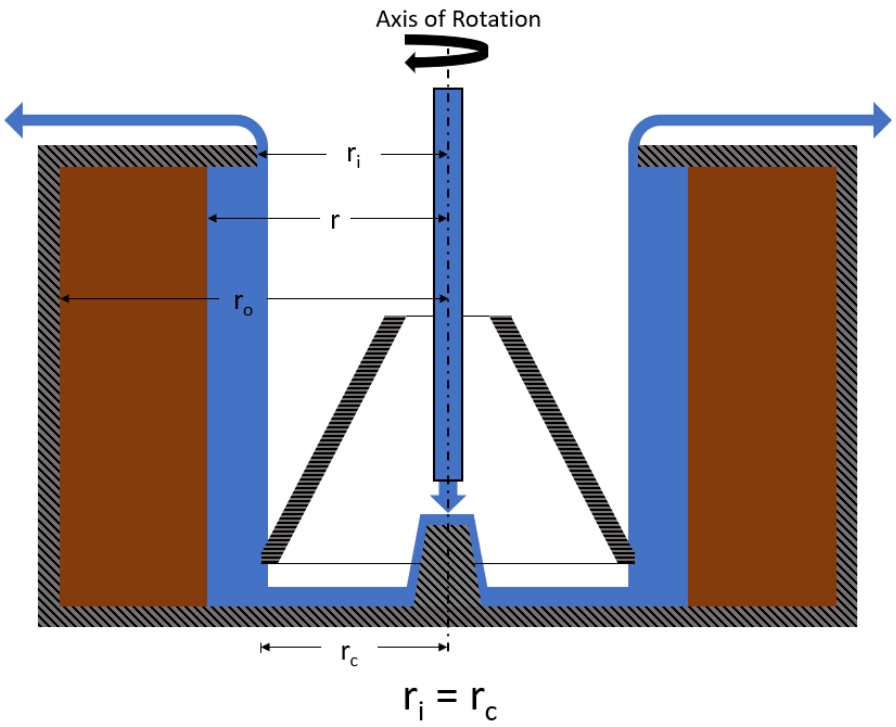

Figure 5-23: Proposed design change of decreasing the feed cone's outer radius to match the inner radius of the weir.

If operating until the bowl is full of solids causes entrainment, another design change that would improve the dewatering of solids is to add holes to the truncated cone which would allow the free water to drain after the batch. This design change would allow for the batch to end once 1 US gal of solids has accumulated and prevent the remaining 0.6 US gal of water mixing with the cake. Depicted in Figure 5-24, the centrifugal force pushes the water away from the holes in the truncated cone during operation and prevents the feed from exiting through them. Once the batch has ended and the centrifugal force has diminished, the free water drains through the holes before it can completely mix with the solids on the wall of the bowl.

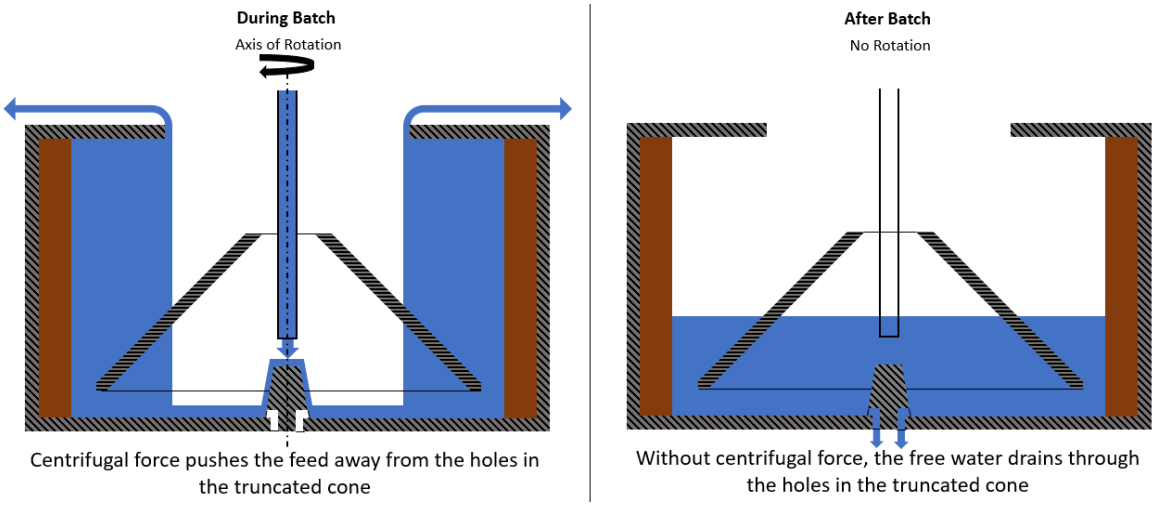

Figure 5-24: Proposed design change of adding drainage hole to the truncated cone. During batch (L) and after batch (R).

5.5 Incineration of Aquaculture Sludge

Instead of being shipped away after centrifugation, another option for disposal is incineration which would not only dispose of the sludge but can also kill pathogens, remove odour, and be used as an energy source.

5.5.1 Incineration of Sludge

Using the HHV and the organic composition of the sludge, the adiabatic flame temperature can be calculated. Both HHV and organic composition are found in Section 5.2. As the wt.% solids of the sludge decreases, the flame temperature gets colder as more energy from combustion is used to evaporate the water within the sludge. The lowest temperature for self-sustaining combustion in an incinerator is about 800°C. To help ensure complete combustion is attained, the solid fuel is burned with 20% excess air (Basu, 2006). Shown in Figure 5-25, it was calculated that the sludge needs to be at a

minimum of 31 wt.% solids to burn at 800°C and any lower solids content would require the addition of another fuel to sustain combustion. A moisture content of 31 wt.% solids was unable to be achieved by centrifugation meaning that sustained combustion is not currently possible without another fuel.

Another option to produce sustained combustion is to start the incinerator with a fuel and then recycle energy from the flue gas to increase the flame temperature to 800°C. However, not all of the energy present in the flue gas can be recycled because as the flue gas temperature decreases, so does the buoyant force that carries it out of the stack. Additionally, the flue gas must be above 150°C to prevent acid from condensing and damaging the stack (French, 1992). By virtue of conservation of energy, the flue gas exhaust temperature after the energy has been extracted is equal to the original adiabatic flame temperature. Seen below in Figure 5-25, the flue gas exhaust temperature is 150°C when the solids content of the sludge is 16 wt.% solids. For this reason, this is the lower limit of a heat recycling system, and a supplemental fuel must be used for incineration when the solids content of the sludge is less than 16 wt.% solids.

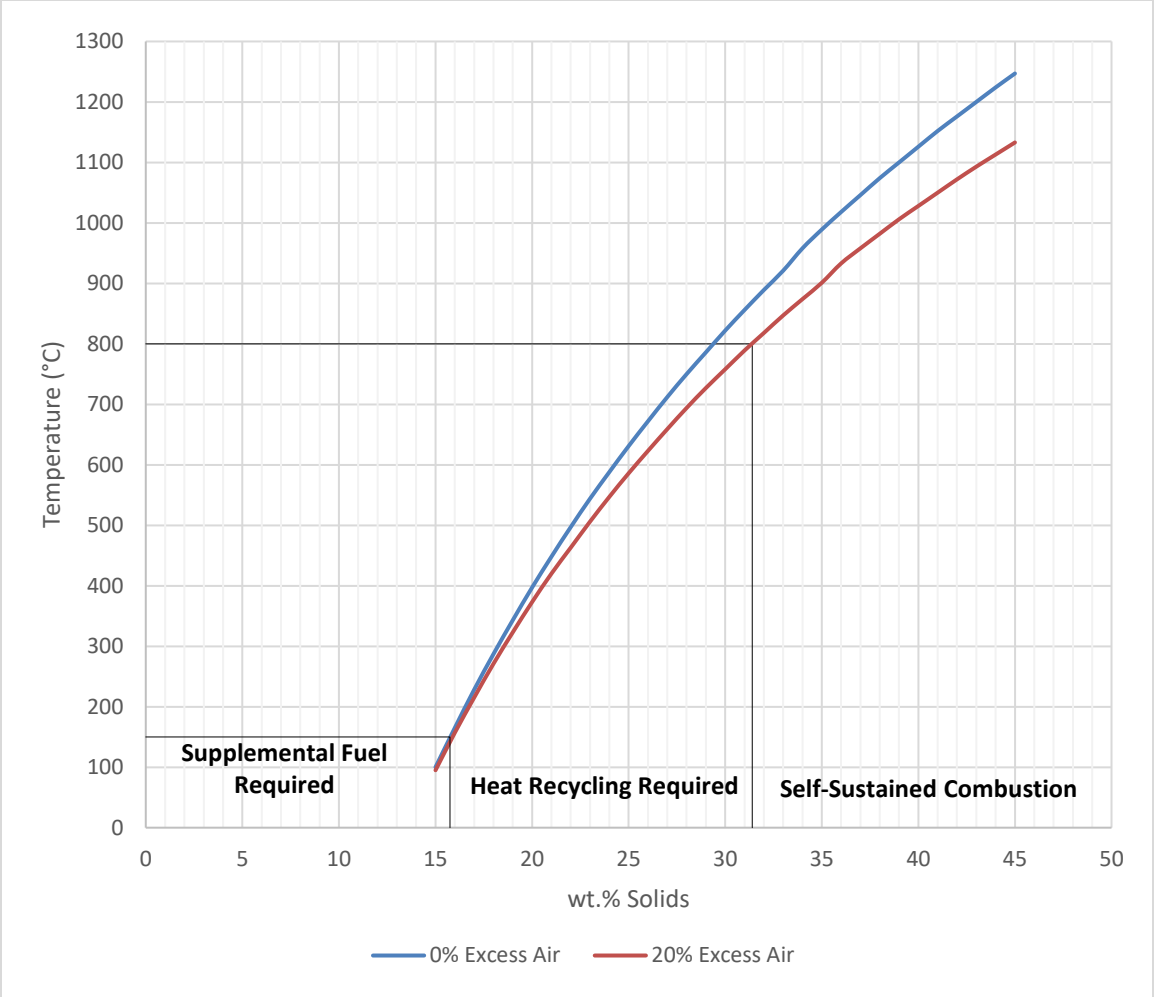

Figure 5-25: Adiabatic flame temperature for the combustion of aquaculture sludge.

A large portion of the energy in the flue gas comes from the evaporation of water, which cannot be recovered above 100°C meaning that the usable energy (sensible heat) in the flue gas is much less than the total energy. As shown in Figure 5-26, when the wt.% solids increase, the percentage of energy required to be extracted from the flue gas decreases and the flue gas exhaust temperature after the energy is recycled increases.

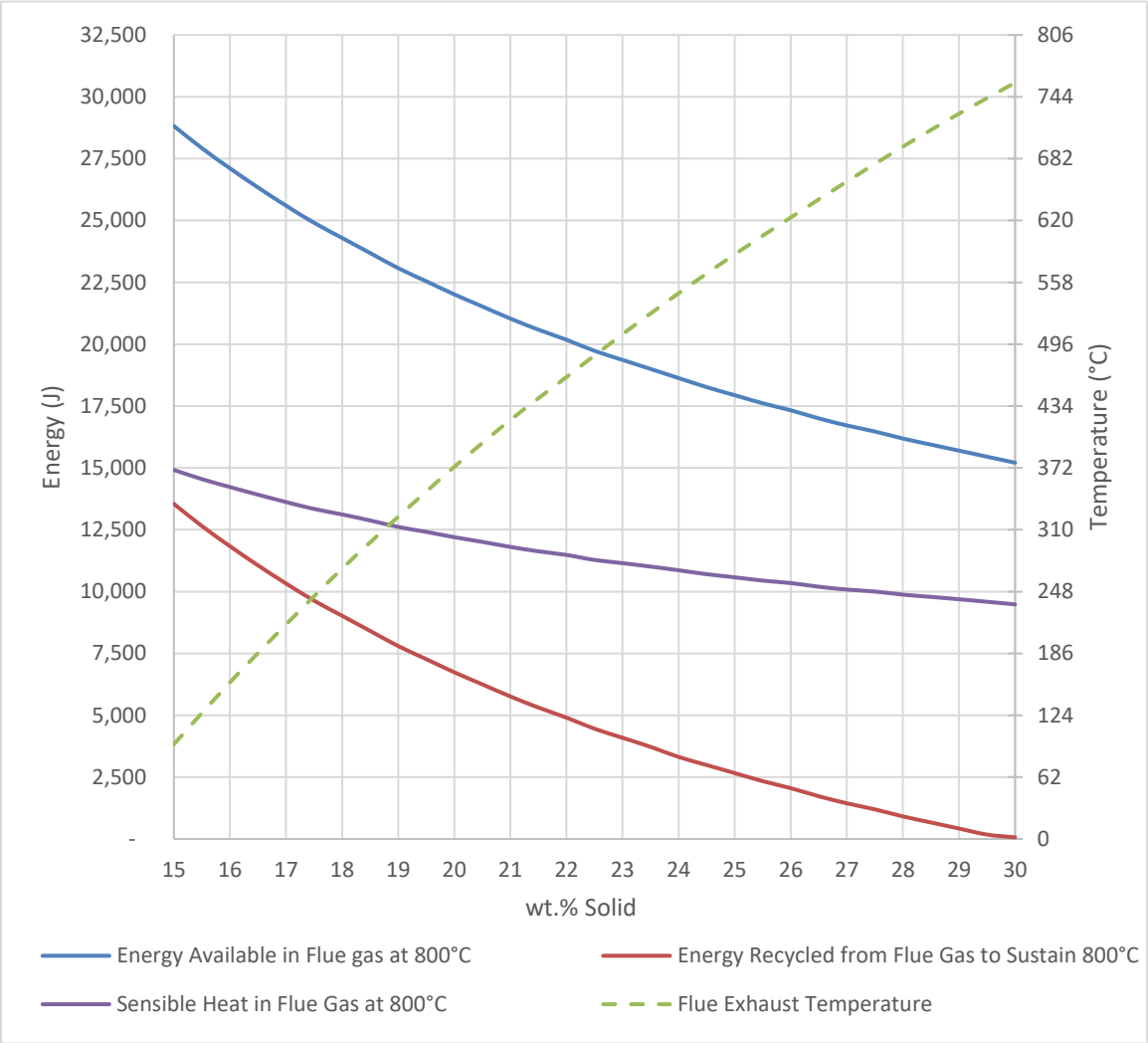

Figure 5-26: Classifications of flue gas energies.

The recovered energy from the flue gas can be utilized by preheating the air entering the incinerator or by drying the incoming sludge. Air preheating alone is not very effective at recycling energy. As shown in Figure 5-27, even if the air is preheated to as high as 500°C, the solids content of the sludge must be in excess of 25 wt.% to achieve flame temperatures above 800°C. Furthermore, expensive metals must be used in the

construction of the air preheater to achieve air temperatures above 300°C as this is beyond the recommended operating temperature for carbon steel.

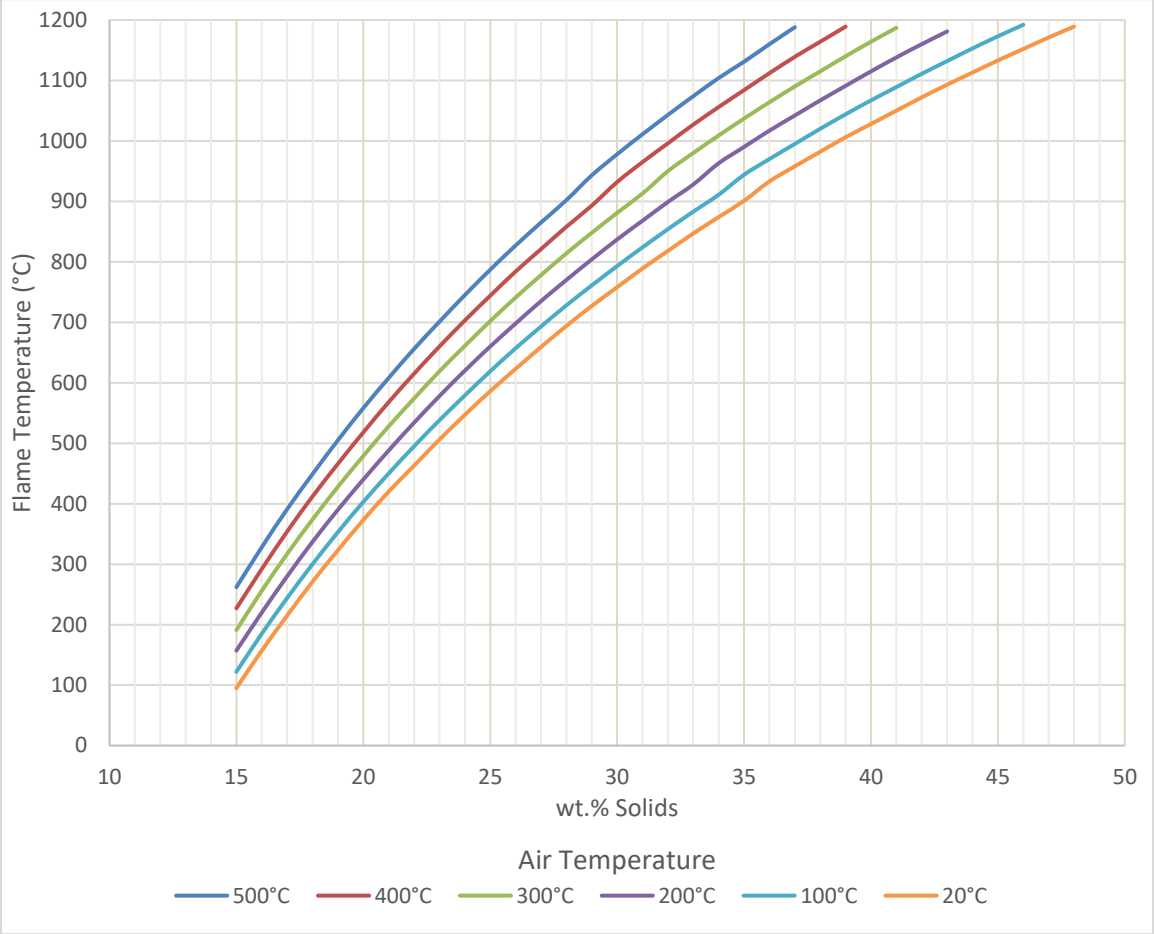

Figure 5-27: Adiabatic flame temperatures with preheated air.

Sludge drying would be done using a screw conveyor heat exchanger. Energy extracted from the flue gas would first be used in a boiler to produce steam. This steam would then be passed through the shaft and/or walls of the screw conveyor carrying the sludge to the incinerator. Heat transferred from the steam would preheat the sludge and evaporate some of its moisture. The evaporated water may contain odorous organic compounds that should not be vented. The evaporated water should instead be fed into the incinerator

with the sludge to destroy any odour causing compounds. As shown below in Figure 5-28, both methods could be used to recycle heat from the flue gas. The flue gas would first pass through a boiler where most of the sensible heat would be used to produce steam that would dry the sludge before returning to the boiler as condensate. The remaining sensible heat in the flue gas would be used to preheat the incoming air before being vented.

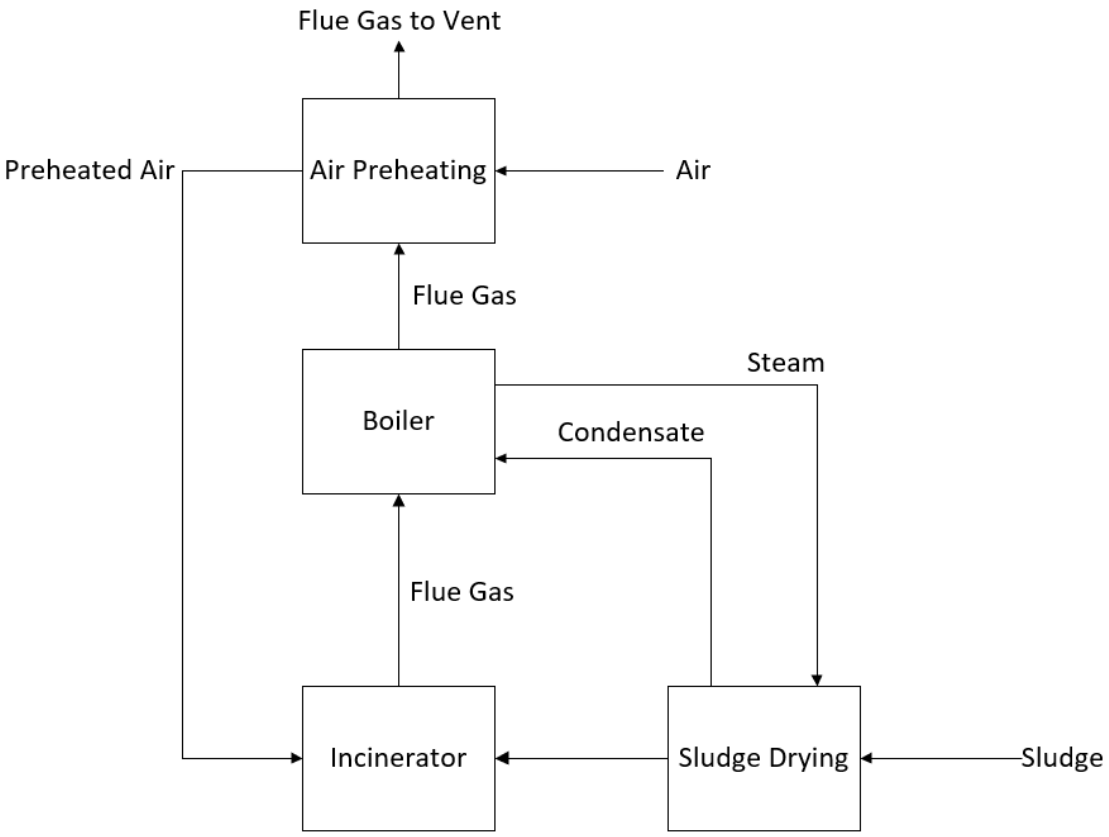

Figure 5-28: Diagram of an incinerator with an air preheating and a sludge drying heat recovery system.

5.5.2 Potential Issues of Sludge Incineration

During the bomb calorimeter test it was noticed that the ash from the sludge fused together to form large spherical particles known as clinkers, which can be seen below in Figure 5-29. Ash fusion occurs when the temperature reaches the melting point for some compounds in the ash. This phenomenon was observed during all trials with all samples of sludge in the bomb calorimeter, however it did not occur during the furnace test which means that clinkers begin to form at some temperature past 550°C. It is likely that the ash fusion can occur in the incinerator at 800°C due to the presence of chlorides in the sludge. Chloride containing compounds such as NaCl, $CaCl_2$, and $MgCl_2$ are found in the sludge and have relatively low melting points of 800°C, 768°C, and 713°C, respectively (Bale, et al., 2016). One advantage of ash fusion in an incinerator is that it reduces fly-ash. By creating larger ash particles, it becomes more difficult for the ash to be carried out of the incinerator with the flue gas and hence reduces the emission of suspended particulate matter. The main drawback of ash fusion is slagging, which is when clinkers fuse to the inside walls and damage the incinerator. To prevent slagging, the sludge would have to be desalinated by a process such as washing, however washing requires large amounts of freshwater.

Another method similar to combustion that can be used to dispose of sludge is pyrolysis, which is the thermal decomposition of organic matter in an oxygen free environment. During pyrolysis, the large complex organic molecules break down to produce bio-oil, solid char, and syngas. Not only would this produce valuable products, but ash slagging would be avoided as pyrolysis occurs between 300-650°C (Basu, 2013).

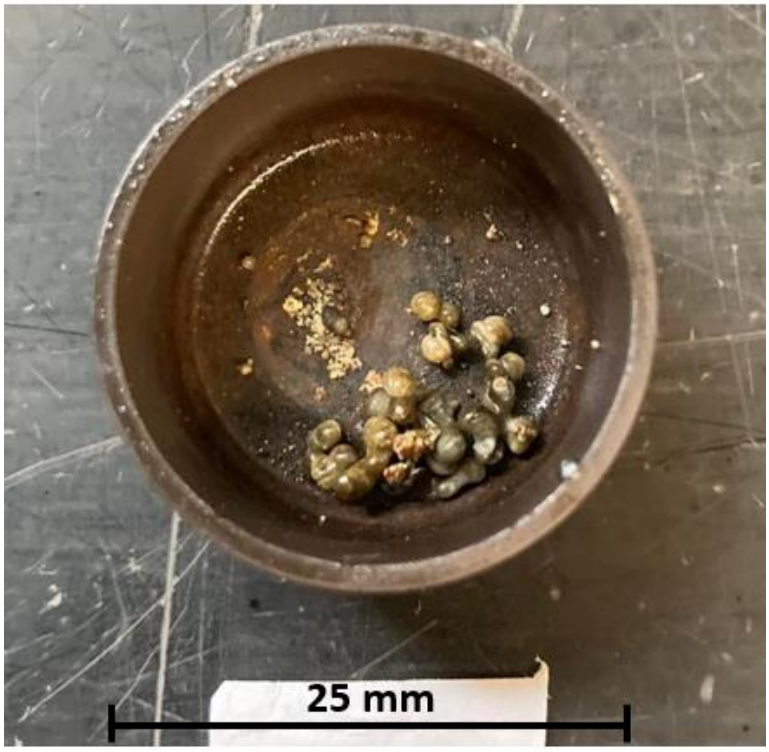

Figure 5-29: Clinkers created from ash fusion during bomb calorimetry tests.

The addition of an incineration process will result in air pollution from the flue gases. It is predicted that the majority of the flue gas will be water vapour which is evaporated from the sludge cake, and N_2 from the air used for combustion. The problematic compounds are NO and SO_2, which are formed during combustion. Fortunately, due to the low nitrogen and sulfur content in the sludge, it is predicted through a mass balance that only 110 g of NO, and 38 g of SO_2 are emitted per kilogram of dry sludge incinerated. It is assumed that the NO is solely produced from the nitrogen in the sludge. This is because the incineration temperature of 800°C is too low for the formation of NO from the oxidation of N_2 in the air. A significant amount of the greenhouse gas CO_2 will be produced, however CO_2 emission from the decomposition of biomass is a part of the natural carbon cycle on earth and does not contribute to climate change.

Chapter 6: Conclusions and Recommendations

6.1 Conclusions

The solids of aquaculture sludge consist of granular particles scattered among viscid material. The viscid material is stringy, mostly organic matter and is difficult to dewater. Meanwhile the granular particles are irregular spheres, flakes, and rods, mostly inorganic and much easier to dewater. The granular particles ranged from a diameter of 25 to 600 μm and had a D_{50} of 400 μm. A particle size analysis could not be performed on the viscid material because the small stringy particles were entangled, and could not be isolated from one another. The granular particles are denser, having a density of 1150 kg/m^3 compared to the 1030 kg/m^3 density of the viscid material.

The ideal dose of chemical conditioners for gravity sedimentation is 150 mg coagulant/g solid and 1 mg flocculant/g solid. This dose promotes settling by creating large flocs and aggregating the microparticles that cause turbidity, but does not improve the dewaterability of sludge by centrifugation. Sludge was dewatered to 19.3 ± 0.7 wt.% solids without chemical conditioners and to 20 ± 1 wt.% solids with chemical conditioners. When sawdust was used as a physical conditioner, the solids content of the centrifuged sludge cake did increase to 23.8 ± 0.3 wt.% solids, however not enough water was lost to overcome the weight gain from adding the sawdust, and the total weight of the cake increased.

The design of the pilot-scale centrifuge did not facilitate dewatering. If operated according to the manufacturer's manual, the unit should be run until there is one US gal of sludge cake in the 1.6 US gal bowl. This results in 0.6 US gal of free water that mixes

with the cake and reduces its solid content to 15 wt.% solids. If operated until the cake completely fills the basket, the sludge can be dewatered to around 23 ± 0.4 wt.% solids, but entrainment of solids in the supernatant is increased to 2.07 ± 0.01 wt.% solids.

The HHV of aquaculture sludge is 16.3 ± 0.2 kJ/g of dry solids. To achieve self-sustained combustion at 800°C, the sludge must contain a minimum of 31 wt.% solids. Sludge with a solids content between 16 to 31 wt.% solids can be incinerated at 800°C if heat from the flue gas is recycled back to the combustor.

6.2 Recommendations

- Adding coagulants and flocculants will not improve dewatering by centrifugation.
- Further research should be performed to determine if breaking the cell walls by heat, chemicals, or sonication will increase dewaterability and if it can be economically implemented on an industrial scale.
- If used as recommended by the manufacturer, a basket centrifuge is not effective at dewatering solids. The design should be modified such that there is no free water remaining in the bowl after the cycle and there is no particle entrainment in the supernatant.
- Further tests should be done to determine if decanter centrifuges can remove water from sludge more effectively than a basket centrifuge.
- For a flue gas heat recovery system, solely preheating the air cannot recycle a sufficient amount energy and as a result, should be combined with sludge drying.

- Before incineration is implemented at hatcheries, additional tests should be performed to determine if slagging and SO_2 and NO emissions will be issues. If so, research into the viability of aquaculture sludge pyrolysis should be pursued.

References

Bale, C. W., Bélise, E., Chartrand, P., Decterov, S. A., Eriksson, G., Gheribi, A. E., . . . Van Ende, M.-A. (2016). FactSage Thermochemical Software and Databases.

Basu, P. (2006). *Combusiton and Gasification in Fluidized Beds.* Boca Raton: Taylor & Francis Group.

Basu, P. (2013). *Biomass Gasification, Pyrolysis and Torrefaction : Practical Design and Theory (2nd Edition).* Amsterdam: Elsevier Inc.

Boxman, S., Kruglick, A., McCarthy, B., Brennan, N., Nystrom, M., Ergas, S., . . . Trotz, M. (2015). Performance evaluation of a commercial land-based integrated multi-trophic aquaculture system using constructed wetlands and geotextile bags for solids treatment. *Aquacultural Engineering*, 23-36.

Cooper, G. M. (2000). *The Cell: A Molecular Approach (2nd Edition).* Sunderland: Sinauer Associates Inc.

Cripps, S., & Bergheim, A. (2000). Solids management and removal for intensive land-based aquaculture production systems. *Aquacultural Engineering*, 33-56.

Davis, M. (2010). *Water and Wastewater Engineering: Design Principles and Practice.* New York: McGraw-Hill.

de Milieux, Z. (2014). *Sludge Dewatering.* Retrieved from SNF Floerger: https://www.snf.com/wp-content/uploads/2019/12/Sludge-Dewatering-EN.pdf

Deng, Y., Dewil, R., Appels, L., Zhang, H., Li, S., & Baeyens, J. (2021). The Need to Accurately Define and Measure the Properties. *Standards*, 19-38.

Ding, A., Qu, F., Liang, H., Guo, S., Ren, Y., Xu, G., & Li, G. (2014). Effect of adding wood chips on sewage sludge. *Royal Chemistry Society Advances*, 24762-24768.

Donaldson, G. (2017). *The Urban Aquaponics Manual - 4th Edition.*

Eppendorf. (2023). *Centrifuge 5804/ 5804 R - Benchtop Centrifuge*. Retrieved from eppendorf: https://online-shop.eppendorf.ca/CA-en/Centrifugation-44533/Multipurpose-Centrifuges-1007184/Centrifuge-5804-5804R-PF-240993.html

French, D. (1992). *Fuel Ash Corrosion.* Retrieved from The National Board of Boiler and Pressure Vessel Inspectors: https://www.nationalboard.org/PrintPage.aspx?pageID=164&ID=196

Generalic, E. (2022, June 29). *Bomb Calorimeter.* Retrieved from Croation-English Chemistry Dictionary & Glossary: https://glossary.periodni.com/glossary.php?en=bomb+calorimeter

Gray, N. (2015). *Progress in Filtreation and Seperation.* Academic Press.

Heidcamp, W. H. (2017). *Cell Biology Laboratory Manual.* Biology Department, Gustavus Adolphus College.

Holman, J. P. (2012). *Experimental Methods for Engineers (8th Edition).* New York: McGraw-Hill.

Islam, M. S., Aryasomayajula, A., & Selvaganapathy, P. (2017). A Review on Macroscale and Microscale Cell Lysis Methods. *Micromachines*, 83-110.

Judd, S. (2020, May 12). *Sludge treatment - propeties of drying sludge.* Retrieved from Sludge Processing: https://www.sludgeprocessing.com/sludge-drying/properties-of-drying-sludge/

Kootenaei, F. G., Mehrdadi, N., Bidhendi, G., Rad, H., Hasanlou, H., & Mahmoudnia, A. (2022). Improvement of Sludge Dewatering by Ultrasonic Pretreatment. *International Journal of Environmental Research*.

Kopp, J., & Dichtl, N. (2001). Influence of the free water content on the dewaterability of sewage . *Water and Science Technology*, 177-183.

Lapple, C. E., & Shepherd, C. B. (1940). Calculation of Particle Trajectories. *Ind. Eng. Chem*, 605-617.

Levenspiel, O. (2014). *Engineering Flow and Heat Exchange.* New York: Springer.

Liu, W., Zhong, X., Cheng, L., Wang, J., Sun, Y., Deng, Y., & Zhang, Z. (2018). Cellular and compositional insight into the sludge dewatering process. *Environmental Science and Pollution Research*, 28942-28953.

Martins, C., Eding, E., Verdegem, M., Heinsbroek, L., Schneider, O., J, B., . . . Verreth, J. (2010). New developments in recirculating aquaculture systems in Europe: A perspective on environmental sustainability. *Aquacultural Enginering*, 83-93.

Patterson, R. N., & Watts, K. C. (2003). Micro-particles in recirculating aquaculture. *Aquacultural Engineering*, 115-130.

Sharrer, M., Rishel, K., Taylor, A., Vinci, B., & Summerfelt, S. (2010). The cost and effectiveness of solids thickening technologies for treating backwash and recovering nutrients from intensive aquaculture systems. *Bioresource Technologies*, 6630-6641.

Svarovsky, L. (2000). *Solid-Liquid Seperation 4th Edition.* Oxford: Butterworth-Heinemann.

Szabó, A., Takács, I., Murphy, S., Daigger, G. T., Licksó, I., & Smith, S. (2008). Significance of design and operational variables in chemical phosphorus removal. *Water Environmental Research*, 407-416.

Timmons, M., Ebeling, J., Wheaton, F., Summerfelt, S., & Vinci, J. (2001). *Recirculating Aquaculture Systems.* Northeastern Regional Aquaculture Center.

US Centrifuge Systems. (2014). *Model M512 Operations Manual.* Retrieved from US Centrifuge Systems.

Vesilind, P. (1994). The role of water in sludge dewatering. *Water Environment Eesearch*, 4-11.

Wakeman, R. (2007). Separation technologies for sludge dewatering. *Journal of Hazardous Materials*, 614-619.

Wei, H., Gao, B., Ren, J., Li, A., & Yang, H. (2018). Coagulation/flocculation in dewatering of sludge: A review. *Water Research*, 608-631.

WRF. (2019). *Tertiary Phosphorus Removal.* Retrieved from The Water Research Foundation: https://www.waterrf.org/sites/default/files/file/2022-09/Tertiary-Phosphorus-Removal.pdf

Yeo, S., Binkowski, F., & Morris, J. (2004). Aquaculture Effluents and Waste By-Products Characteristics, Potential Recovery, and Beneficial Reuse. *North Central Regional Aquaculture Center*.

Zhang, X., Kang, H., Zhang, Q., Hao, X., Han, X., & Zhang, W. (2019). The porous structure effects of skeleton builders in sustainable sludge. *Environmental Management*, 14-20.

Appendix A: Complete Trace Metal Analysis Results

Table A-1: Results from the trace metal analysis tests performed by the Research and Productivity Council of Fredericton.

Analytes	Units	Adult Broodstock	Young Broodstock	Granular	Viscid
Aluminum	mg/kg	608	270	148	130
Antimony	mg/kg	0.2	< 0.1	< 0.1	< 0.1
Arsenic	mg/kg	3	2	2	3
Barium	mg/kg	40	25	24	16
Beryllium	mg/kg	< 0.1	< 0.1	< 0.1	< 0.1
Bismuth	mg/kg	< 1	< 1	< 1	< 1
Boron	mg/kg	14	4	5	6
Cadmium	mg/kg	1.37	1.54	1.89	1.59
Calcium	mg/kg	79,900	109,000	183,000	66,700
Chromium	mg/kg	6	2	2	2
Cobalt	mg/kg	24.1	9.2	1.1	0.8
Copper	mg/kg	87	33	27	55
Iron	mg/kg	4,630	1,310	810	740
Lead	mg/kg	5.3	0.9	0.6	0.7
Lithium	mg/kg	1.2	2.1	1.4	0.5
Magnesium	mg/kg	4,720	3,160	4,430	3,380
Manganese	mg/kg	448	189	242	148
Molybdenum	mg/kg	1.2	0.7	0.6	0.8
Nickel	mg/kg	6	1	1	2
Potassium	mg/kg	1390	310	340	560
Rubidium	mg/kg	0.7	0.4	0.2	0.3
Selenium	mg/kg	2	2	< 1	2
Silver	mg/kg	0.5	< 0.1	< 0.1	< 0.1
Sodium	mg/kg	12,300	2,780	4,630	9,940
Strontium	mg/kg	214	317	240	120
Tellurium	mg/kg	< 0.1	< 0.1	< 0.1	< 0.1
Thallium	mg/kg	< 0.1	< 0.1	< 0.1	< 0.1
Tin	mg/kg	< 1	< 1	< 0.1	< 0.1
Uranium	mg/kg	1.2	0.2	0.4	0.4
Vanadium	mg/kg	3	2	5	4
Zinc	mg/kg	986	837	722	664

Appendix B: Experimental Data

Table B-1: Density of dry sludge by liquid displacement.

Solid Type	Density (g/cm3)	Average	Std.Dev
Viscid Material	1.211	1.216	0.007
	1.221		
Granular Particles	1.647	1.57	0.07
	1.567		
	1.503		

Table B-2: HHV of sludge samples.

Sludge Type	HHV (kJ/g)	Average	Std.Dev
Adult Broodstock	16.66	16.4	0.3
	16.23		
	16.16		
Young Broodstock	16.35	16.3	0.1
	16.13		
	16.37		
Granular Particles	8.00	8.6	0.8
	9.18		
Viscid Material	24.19	24.0	0.3
	23.81		

Table B-3: Turbidity of adult broodstock sludge that has been dosed with coagulants

Dose (mg/g Solid)		Turbidity (FAU)
FS	0	208
	41	50.5
	164	28
	327	54
	463	58.5
PAC	0	230
	75	36
	149	17
	223	74
	297	85

Table B-4: Turbidity of shredded adult broodstock sludge that has been dosed with a coagulant.

PAC (mg/g Solid)	Turbidity (FAU)
0	896
74	204
149	90
223	54
297	108

Table B-5: Turbidity of adult broodstock sludge of various TSS that has been dosed with coagulants.

TSS (mg/L)	FS (mg/g Solid)	Turbidity (FAU)	% Reduction
9,900	0	523	0%
	48	278	47%
	157	110	79%
	307	122	77%
	477	139	73%
4,600	0	351	0%
	41	98	72%
	164	47	87%
	313	69	80%
	477	76	78%
2,500	0	208	0%
	41	51	76%
	164	28	87%
	327	54	74%
	463	59	72%

Table B-6: Turbidity of adult broodstock sludge that has been dosed with FS and PAM.

PAM (mg/g Solid)	FS (mg/g Solid)	Turbidity (FAU)
0	0	126
0	74	49
0	149	32
0	223	68
0	297	126
1	0	126
1	74	39
1	149	21
1	223	40
1	297	99
3	0	126
3	74	27
3	149	15
3	223	11
3	297	31
5	0	126
5	74	31
5	149	18
5	223	14
5	297	18
10	0	126
10	74	37
10	149	21
10	223	17
10	297	19
15	0	126
15	74	37
15	149	22
15	223	18
15	297	19

Table B-7: Turbidity of adult broodstock sludge that has been dosed with PAC and PAM.

PAM (mg/g Solid)	PAC (mg/g Solid)	Turbidity (FAU)
0	0	230
0	74	36
0	149	28
0	223	74
0	297	85
1	0	230
1	74	30
1	149	21
1	223	19
1	297	63
3	0	230
3	74	31
3	149	14
3	223	13
3	297	22
5	0	230
5	74	33
5	149	15
5	223	16
5	297	14
10	0	230
10	74	36
10	149	21
10	223	17
10	297	12
15	0	230
15	74	39
15	149	21
15	223	19
15	297	12

Table B-8: Turbidity of shredded adult broodstock sludge that has been dosed with PAC and PAM.

PAM (mg/g Solid)	PAC (mg/g Solid)	Turbidity (FAU)
0	0	896
0	74	204
0	149	90
0	223	54
0	297	108
1	0	896
1	74	193
1	149	78
1	223	49
1	297	70
5	0	896
5	74	92
5	149	75
5	223	50
5	297	39
10	0	896
10	74	88
10	149	74
10	223	50
10	297	49
15	0	896
15	74	86
15	149	76
15	223	51
15	297	39

Table B-9: Solid content of young broodstock sludge that has been centrifuged at various RCF.

RCF (g-force)	wt.% Solids	Average	Std. Dev
1	9.70%	9.62%	0.07%
	9.59%		
	9.56%		
500	17.01%	16.7%	0.3%
	16.43%		
	16.72%		
1000	19.08%	18.4%	0.6%
	17.82%		
	18.39%		
1500	19.62%	19.3%	0.3%
	19.32%		
	19.04%		
2000	19.30%	20.0%	0.6%
	20.22%		
	20.32%		
2500	20.22%	20.0%	0.5%
	20.46%		
	19.42%		
3000	20.54%	20.4%	0.5%
	19.93%		
	20.82%		

Table B-10: Solid content of young broodstock sludge that has been centrifuged at various batch times.

Time (Min)	wt.% Solids	Average	Std. Dev
0	7.17%	7.3%	0.2%
	7.15%		
	7.40%		
	7.58%		
5	17.12%	17.0%	0.2%
	16.98%		
	16.74%		
10	18.07%	18.5%	0.4%
	18.68%		
	18.84%		
15	19.57%	19.8%	0.3%
	19.65%		
	20.04%		
20	19.90%	19.9%	0.1%
	19.86%		
	20.06%		
30	19.66%	19.9%	0.2%
	20.09%		
	20.06%		

Table B-11: Solids content of adult broodstock sludge that has been centrifuged at 2,500 g-force for 20 min.

Day	Raw Sludge			Chemically Treated Sludge		
	wt.% Solids	Average	Std. Dev	wt.% Solids	Average	Std. Dev
1	19.27%	19.3%	0.7%	21.92%	20%	1%
	18.28%			21.26%		
	18.58%			22.19%		
2	18.89%			18.66%		
	19.39%			18.73%		
	19.44%			19.41%		
3	19.03%			18.13%		
	19.32%			18.17%		
	19.44%			18.28%		
4	19.09%			19.26%		
	19.62%			19.34%		
	19.68%			19.07%		
5	19.99%			20.35%		
	19.95%			20.35%		
	19.57%			20.42%		
6	20.32%			20.79%		
	20.31%			20.49%		
	20.38%			21.55%		
7	18.13%			20.80%		
	18.17%			21.54%		
	18.28%			21.37%		

Table B-12: Solids content of adult broodstock sludge that has been centrifuged at 2,500 g-force for 20 min

Cake Location	wt.% Solids	Average	Std.Dev
Entire	19.23%	18.8%	0.4%
	19.14%		
	18.74%		
	19.10%		
	18.43%		
	18.56%		
	18.21%		
Top	9.34%	9.1%	0.3%
	9.12%		
	8.74%		
Bottom	36.38%	38%	2%
	38.47%		
	39.65%		

Table B-13: Solid content of sludge from the bottom and the top of the septic tank that has been centrifuged at 2,500 g-force for 20 min.

Sample Depth	wt.% Solids	Average	Std.Dev
0 m (Surface)	19.75%	19.5%	0.8%
	20.13%		
	18.62%		
2.45 m (Bottom)	33.37%	33.9%	0.5%
	34.42%		
	33.89%		

Table B-14: Concentration of orthophosphate in the supernatant.

Sludge	Orthophosphates in Supernatant (ppm)	Average	Std.Dev
Young Broodstock Sludge	120	125	22
	115		
	157.7		
	107.5		
Coagulated Sludge	133.2	124	13
	115		

Table B-15: Solids content of young broodstock sludge and sawdust that has been centrifuged at 2,500 g-force for 20 min.

Ratio (Dry SD: Dry Sludge)	g of Sawdust	g of Dry Sawdust	g dry Sludge	wt.% Solid	Average	Std. Dev
0:1	0	0.000	4.219	20.32%	20.34%	0.04%
				20.31%		
				20.38%		
1:8	0.632	0.528	4.234	21.37%	21.21%	0.26%
				21.35%		
				20.91%		
1:4	1.261	1.054	4.061	24.16%	23.71%	0.44%
				23.27%		
				23.69%		
1:2	2.51	2.098	3.959	23.94%	23.91%	0.11%
				23.79%		
				23.99%		
1:1	6.048	4.191	4.162	23.83%	23.93%	0.38%
				24.35%		
				23.60%		

Table B-16: Solid content of shredded young broodstock sludge that has been centrifuged at 2,500 g-force for 20 min.

Sludge Condition	wt.% Solids	Average	Std.Dev
Shredded	11.00%	10.9%	0.3%
	10.57%		
	11.05%		
Shredded + Re-flocculated	15.72%	16.0%	0.2%
	16.15%		
	16.03%		

Table B-17: Mass and solids content of young broodstock sludge recorded during the mass balance on the basket centrifuge.

Location	Weight (kg)	wt.% Solids	Average	Std.Dev
Feed	20.08	10.94%	9%	1%
		7.29%		
		8.27%		
		8.53%		
		10.53%		
		7.80%		
Bowl	6.5	23.24%	23.1%	0.4%
		23.47%		
		22.72%		
Supernatant	12.75	2.06%	2.07%	0.01%
		2.06%		
		2.08%		

Appendix C: Propagation of Error When Determining the Weight Fraction of Granular Particles

To determine the mass fraction of granular particles in dry aquaculture sludge (x), the HHV carbon, hydrogen, and fixed solid of its components were used. Equation (C-1) describes aquaculture sludge (S) as being composed of granular particles (G) and viscid material (V). To solve for x, Equation (C-1) can be rearranged to Equation (C-2).

$$S = xG + (1 - x)V \quad \textbf{(C-1)}$$

$$x = \frac{(S-V)}{(G-V)} \quad \textbf{(C-2)}$$

Each independent variable in Equation (C-2) has some degree of uncertainty (σ) which propagates through the equation and results in x also having an uncertainty. The error for x can be determined by using the propagation of uncertainty formula shown below in Equation (C-3) (Holman, 2012). The solutions for the partial derivative of the function x with respect to its independent variables S, G, and V can be seen in Equations (C-4), (C-5), and (C-6), respectively.

$$\sigma_x^2 = \left(\frac{\partial x}{\partial S}\right)_{G,V}^2 \sigma_S^2 + \left(\frac{\partial x}{\partial G}\right)_{S,V}^2 \sigma_G^2 + \left(\frac{\partial x}{\partial V}\right)_{S,G}^2 \sigma_S^2 \quad \textbf{(C-3)}$$

$$\left(\frac{\partial x}{\partial S}\right)_{G,V} = \frac{\partial}{\partial S}\frac{(S-V)}{(G-V)} = \frac{1}{G-V} \quad \textbf{(C-4)}$$

$$\left(\frac{\partial x}{\partial G}\right)_{S,V} = \frac{\partial}{\partial G}\frac{(S-V)}{(G-V)} = \frac{V-S}{(G-V)^2} \quad \textbf{(C-5)}$$

$$\left(\frac{\partial x}{\partial V}\right)_{S,G} = \frac{\partial}{\partial V}\frac{(S-V)}{(G-V)} = \frac{S-G}{(G-V)^2} \quad \textbf{(C-6)}$$

Equation (C-7) can be used to calculate σ_x, and is derived by combining Equations (C-3), (C-4), (C-5), and (C-6).

$$\sigma_x = \sqrt{\left(\frac{1}{G-V}\right)^2 \sigma_S^2 + \left(\frac{V-S}{(G-V)^2}\right)^2 \sigma_G^2 + \left(\frac{S-G}{(G-V)^2}\right)^2 \sigma_S^2} \quad \textbf{(C-7}$$

Curriculum Vitae

Candidate’s full name: Alex Mann

Universities attended: BScE in Chemical Engineering, University of New Brunswick, 2021

Publications: N/A

Conference Presentation: N/A